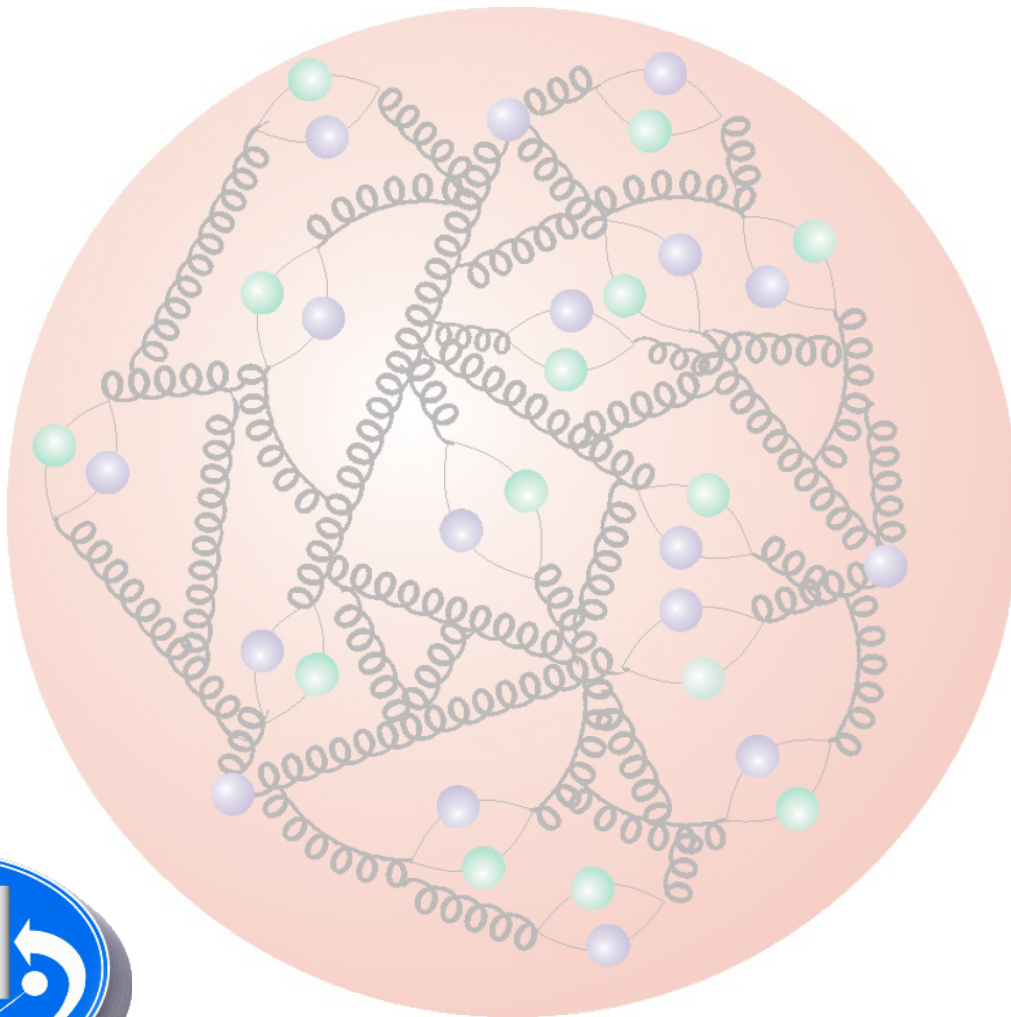


Proton Structure Measurements from HERA



Deep Inelastic Scattering
H1 , ZEUS & HERA ep Collider
Data Combination
QCD Analyses & HERAPDF2.0
Conclusions



HepMad - Antananarivo - Madagascar
September 2015

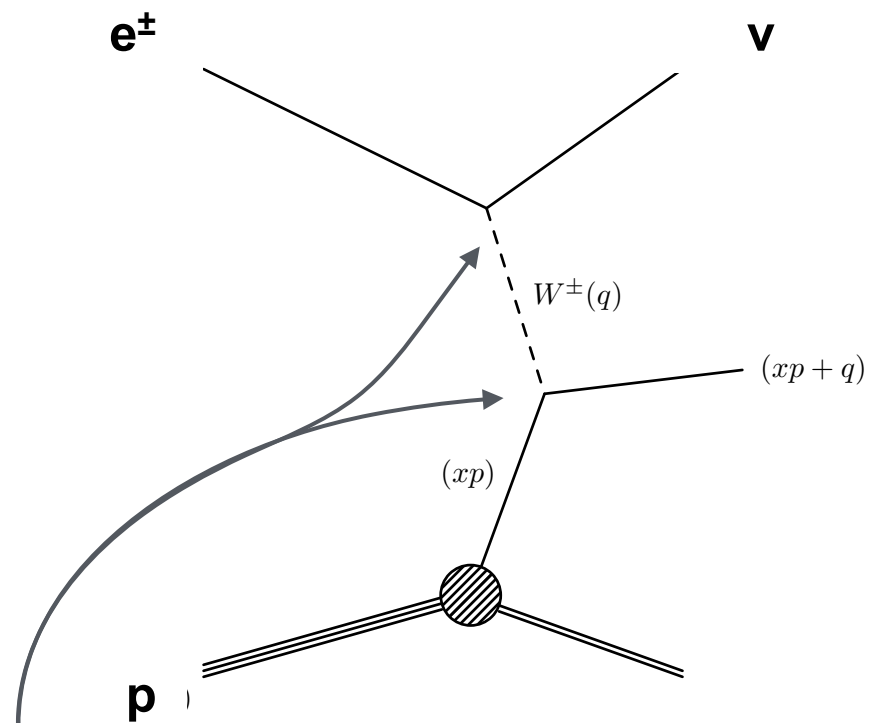
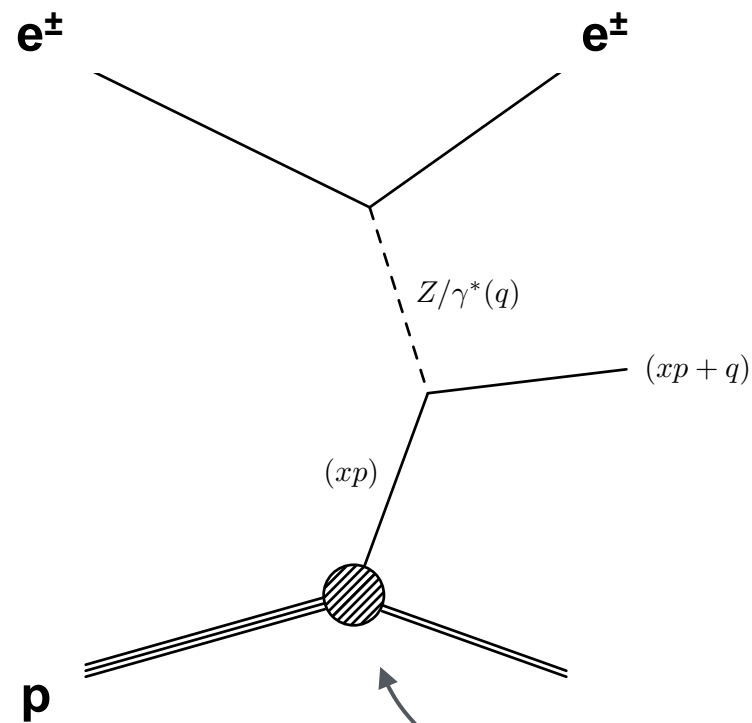


Eram Rizvi

Queen Mary
University of London

Neutral current scattering

Charged current scattering



Factorisation in ep collisions: $\sigma_{ep \rightarrow eX} = f_{p \rightarrow i} \otimes \hat{\sigma}_{ei \rightarrow eX}$

$xf_{p \rightarrow i}$ = quark / gluon momentum density in proton:
parton density function (PDFs)

Use factorisation in pp collisions at LHC: $\sigma_{pp \rightarrow X} = f_{p \rightarrow i} \otimes \hat{\sigma}_{i,j \rightarrow X} \otimes f_{p \rightarrow j}$

Signature
Isolated electron/positron
pT balanced with hadronic system X

Signature
No detected lepton (neutrino)
pT imbalanced for hadronic system X

PDFs are not observables - only structure functions are
Measuring these cross sections allows indirect access to the universal PDFs $xf_{p \rightarrow i}$

$$\frac{d\sigma_{NC}^{\pm}}{dx dQ^2} = \frac{2\pi\alpha^2}{x} \left[\frac{1}{Q^2} \right]^2 \left[Y_+ \tilde{F}_2 \mp Y_- x \tilde{F}_3 - y^2 \tilde{F}_L \right]$$

$$\frac{d\sigma_{CC}^{\pm}}{dx dQ^2} = \frac{G_F^2}{4\pi x} \left[\frac{M_W^2}{M_W^2 + Q^2} \right]^2 \left[Y_+ \tilde{W}_2^{\pm} \mp Y_- x \tilde{W}_3^{\pm} - y^2 \tilde{W}_L^{\pm} \right]$$

$$Y_{\pm} = 1 \pm (1-y)^2$$

$$\tilde{F}_2 \propto \sum (xq_i + x\bar{q}_i)$$

Dominant contribution

$$x\tilde{F}_3 \propto \sum (xq_i - x\bar{q}_i)$$

Only sensitive at high $Q^2 \sim M_Z^2$

$$\tilde{F}_L \propto \alpha_s \cdot xg(x, Q^2)$$

Only sensitive at low Q^2 and high y

The NC reduced cross section defined as:

$$\tilde{\sigma}_{NC}^{\pm} = \frac{Q^2 x}{2\alpha\pi^2} \frac{1}{Y_+} \frac{d^2\sigma^{\pm}}{dx dQ^2}$$

$$\tilde{\sigma}_{NC}^{\pm} \sim \tilde{F}_2 \mp \frac{Y_-}{Y_+} x\tilde{F}_3$$

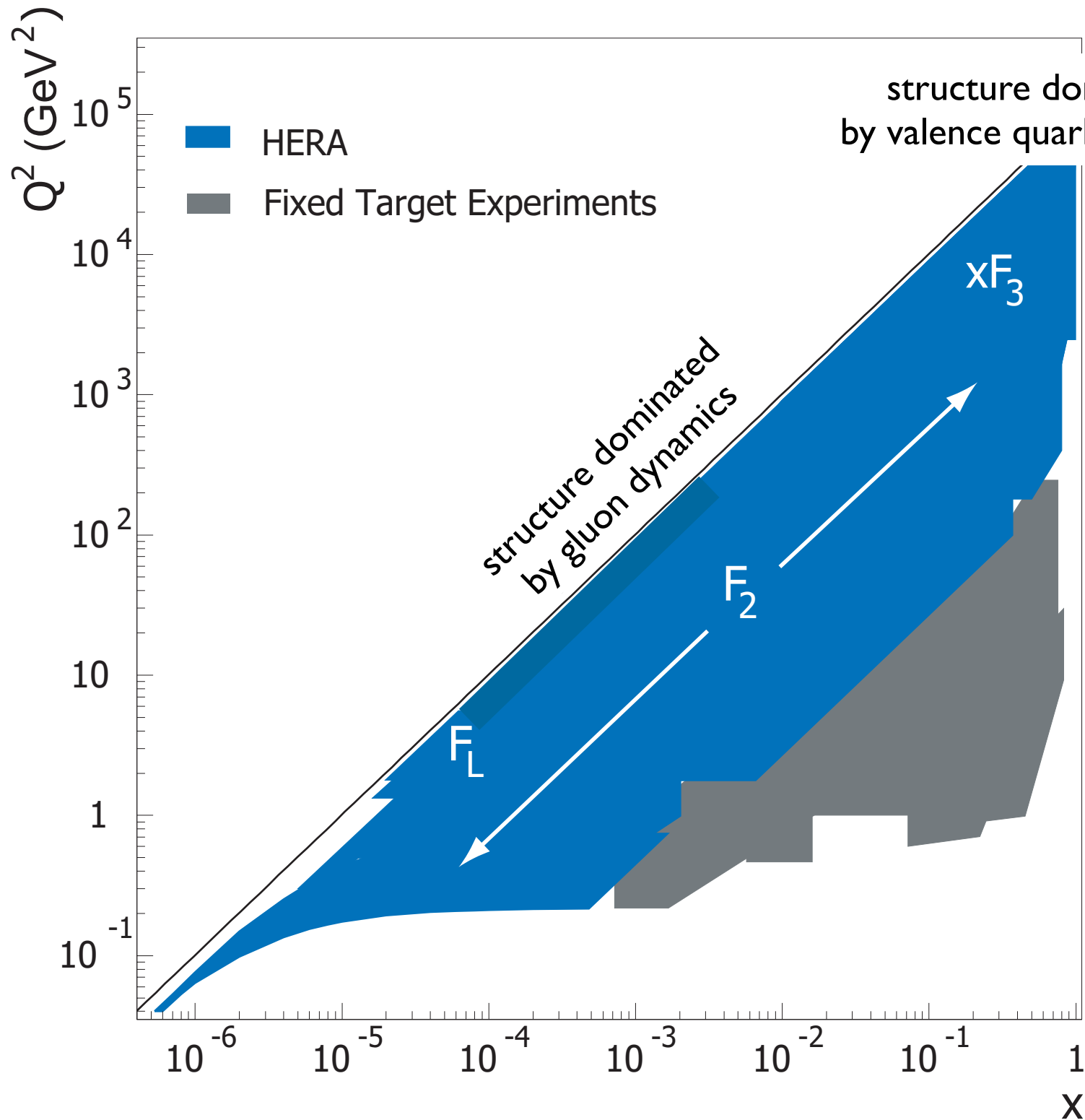
The CC reduced cross section defined as:

$$\sigma_{CC}^{\pm} = \frac{2\pi x}{G_F^2} \left[\frac{M_W^2 + Q^2}{M_W^2} \right]^2 \frac{d\sigma_{CC}^{\pm}}{dx dQ^2}$$

$$\frac{d\sigma_{CC}^{\pm}}{dx dQ^2} = \frac{1}{2} \left[Y_+ W_2^{\pm} \mp Y_- x W_3^{\pm} - y^2 W_L^{\pm} \right]$$

similarly for pure weak CC analogues:

$$W_2^{\pm}, xW_3^{\pm} \text{ and } W_L^{\pm}$$



HERA data cover wide region of x, Q^2

Q^2 = boson virtuality

x = fractional momentum of struck quark

NC Measurements

F_2 dominates most of Q^2 reach

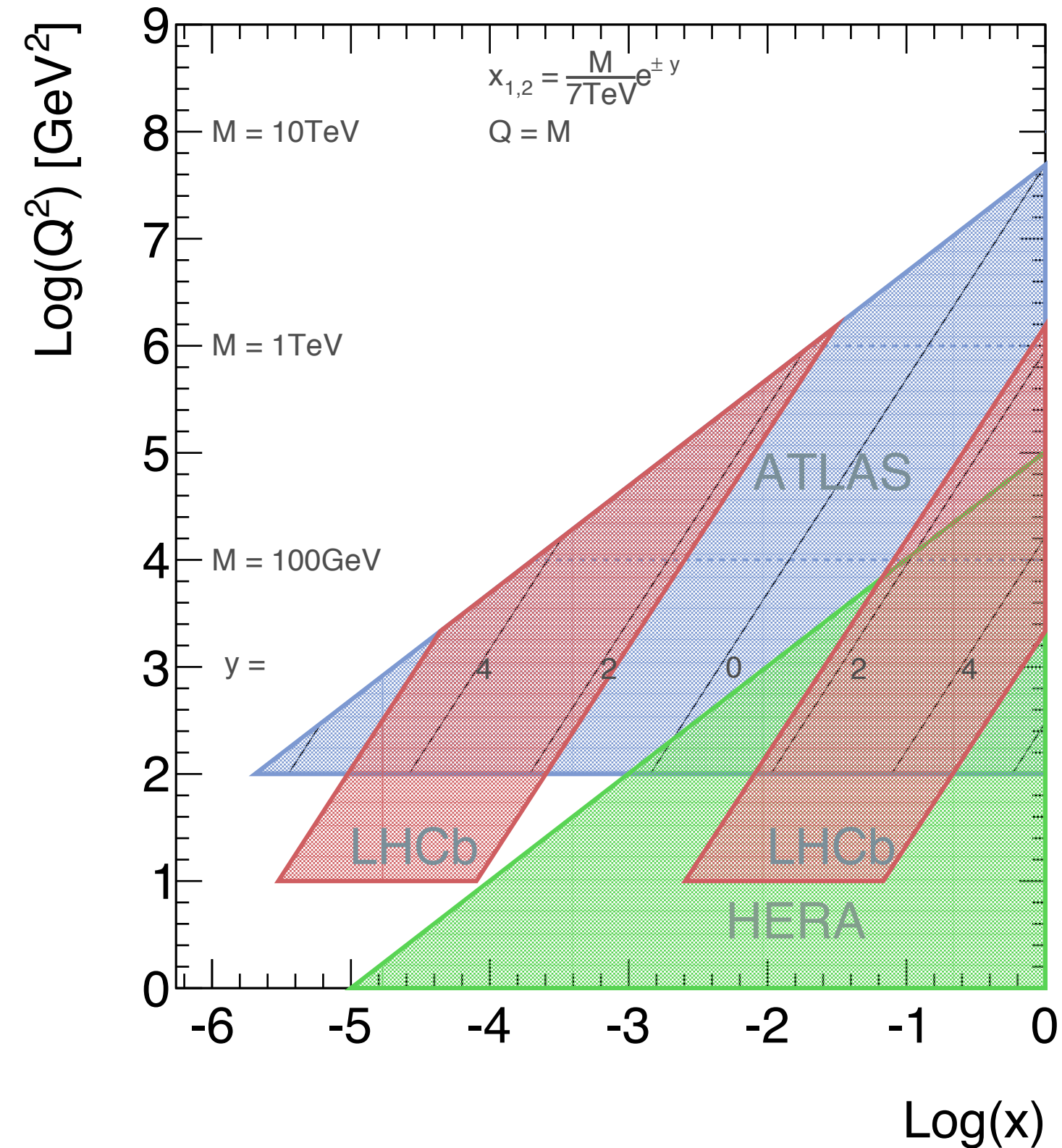
xF_3 contributes in EW regime

F_L contributes only at highest y

CC Measurements

W_2 and xW_3 contribute equally

W_L only at high y



LHC: largest mass states at large x

For central production $x=x_1=x_2$

$$M=x\sqrt{s}$$

i.e. $M > 1\text{ TeV}$ probes $x > 0.1$

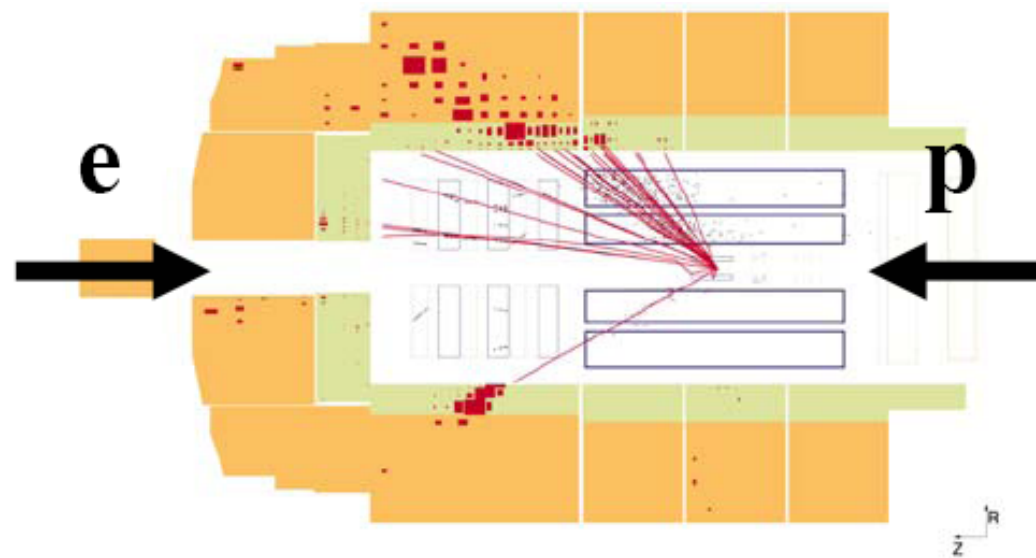
Searches for high mass states require precision knowledge at high x

Z' / quantum gravity / susy searches...

DGLAP evolution allows predictions to be made

High x predictions rely on

- data (DIS / fixed target)
- sum rules
- behaviour of PDFs as $x \rightarrow 1$



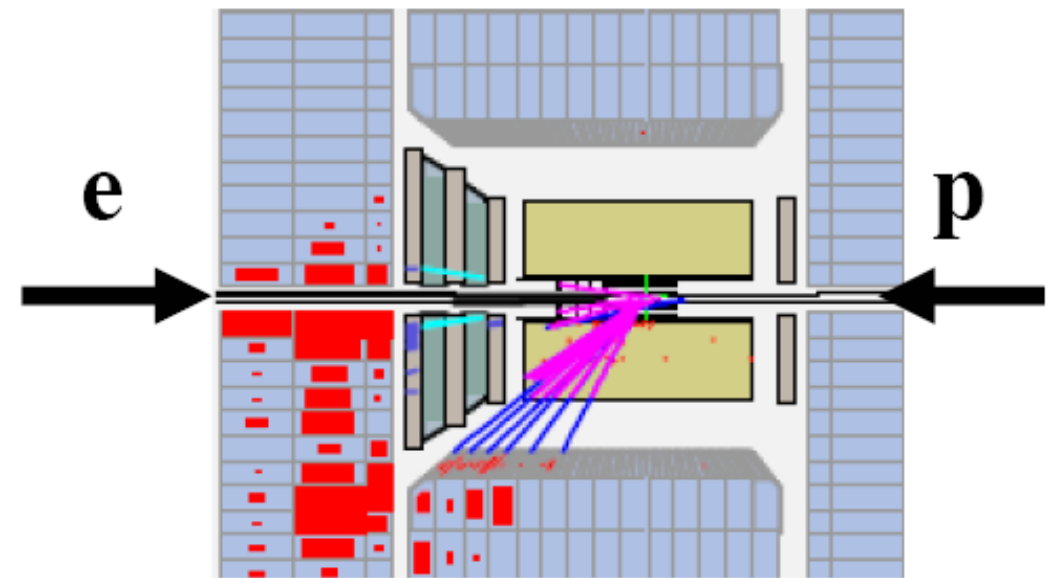
Neutral current event selection:

High P_T isolated scattered lepton
 Suppress huge photo-production background by imposing longitudinal energy-momentum conservation

Kinematics may be reconstructed in many ways:
 energy/angle of hadrons & scattered lepton
 provides excellent tools for sys cross checks

Removal of scattered lepton provides a high stats “pseudo-charged current sample”
 Excellent tool to cross check CC analysis

Final selection: $\sim 10^5$ events per sample at high Q^2
 $\sim 10^7$ events for $10 < Q^2 < 100 \text{ GeV}^2$



Charged current event selection:

Large missing transverse momentum (neutrino)
 Suppress huge photo-production background
 Topological finders to remove cosmic muons
 Kinematics reconstructed from hadrons
 Final selection: $\sim 10^3$ events per sample

HERA-I operation 1993-2000

$E_e = 27.6 \text{ GeV}$

$E_p = 820 / 920 \text{ GeV}$

$\sqrt{s} = 301 \text{ GeV} \ \& \ \sqrt{s} = 318 \text{ GeV}$

$\int \mathcal{L} \sim 110 \text{ pb}^{-1}$ per experiment

HERA-II operation 2003-2007

$E_e = 27.6 \text{ GeV}$

$E_p = 920 \text{ GeV}$

$\sqrt{s} = 318 \text{ GeV}$

$\int \mathcal{L} \sim 330 \text{ pb}^{-1}$ per experiment

Longitudinally polarised leptons

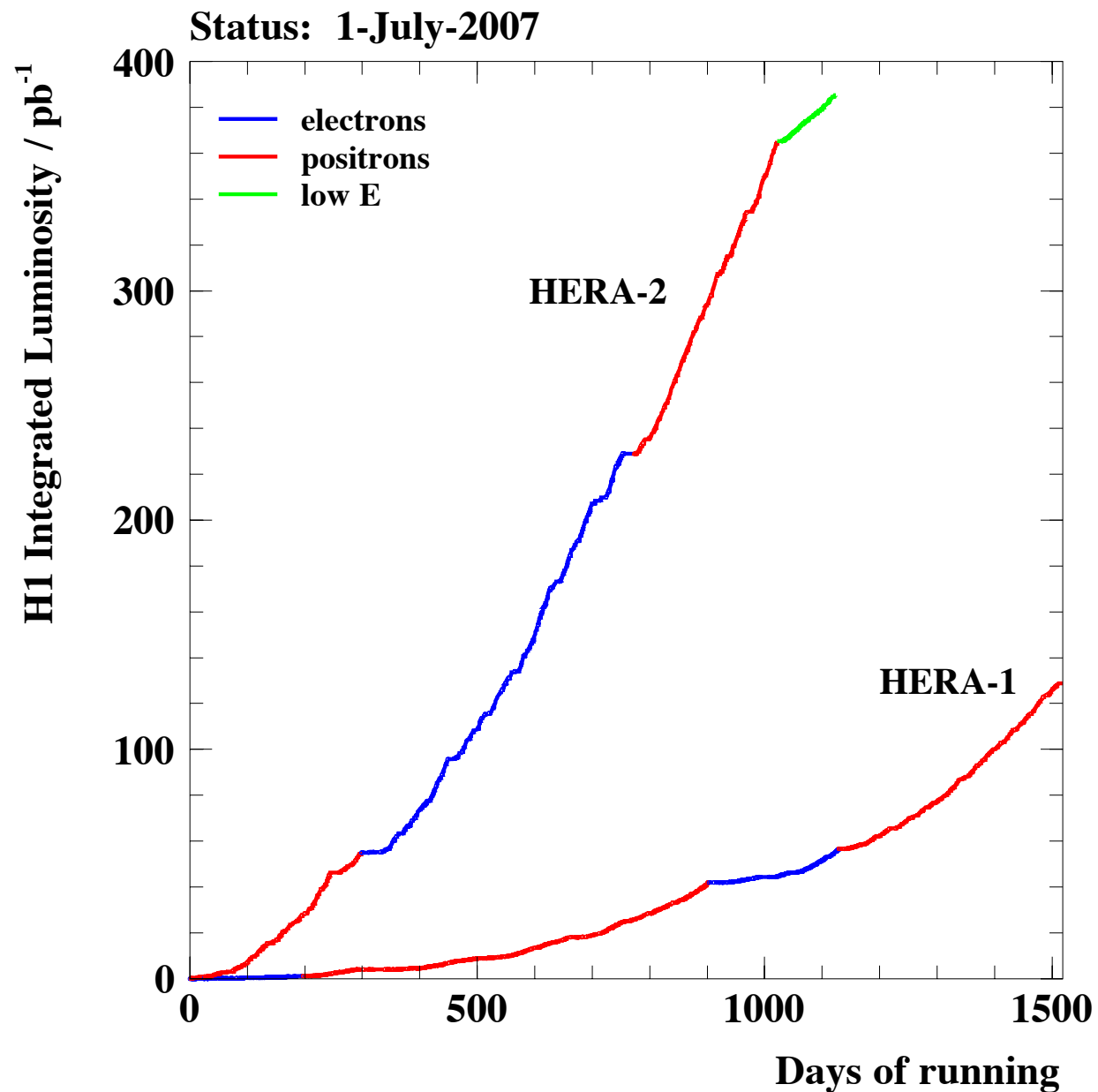
Low Energy Run 2007

$E_e = 27.6 \text{ GeV}$

$E_p = 575 \ \& \ 460 \text{ GeV}$

$\sqrt{s} = 225 \text{ GeV} \ \& \ \sqrt{s} = 251 \text{ GeV}$

Dedicated F_L measurement





Summary of HERA-I datasets Combined in HERAPDF1.0

Available since 2009

Data Set		x Range		Q^2 Range GeV ²		\mathcal{L} pb ⁻¹	e^+/e^-	\sqrt{s} GeV
H1 svx-mb	95-00	5×10^{-6}	0.02	0.2	12	2.1	$e^+ p$	301-319
H1 low Q^2	96-00	2×10^{-4}	0.1	12	150	22	$e^+ p$	301-319
H1 NC	94-97	0.0032	0.65	150	30000	35.6	$e^+ p$	301
H1 CC	94-97	0.013	0.40	300	15000	35.6	$e^+ p$	301
H1 NC	98-99	0.0032	0.65	150	30000	16.4	$e^- p$	319
H1 CC	98-99	0.013	0.40	300	15000	16.4	$e^- p$	319
H1 NC HY	98-99	0.0013	0.01	100	800	16.4	$e^- p$	319
H1 NC	99-00	0.0013	0.65	100	30000	65.2	$e^+ p$	319
H1 CC	99-00	0.013	0.40	300	15000	65.2	$e^+ p$	319
ZEUS BPC	95	2×10^{-6}	6×10^{-5}	0.11	0.65	1.65	$e^+ p$	301
ZEUS BPT	97	6×10^{-7}	0.001	0.045	0.65	3.9	$e^+ p$	301
ZEUS SVX	95	1.2×10^{-5}	0.0019	0.6	17	0.2	$e^+ p$	301
ZEUS NC	96-97	6×10^{-5}	0.65	2.7	30000	30.0	$e^+ p$	301
ZEUS CC	94-97	0.015	0.42	280	17000	47.7	$e^+ p$	301
ZEUS NC	98-99	0.005	0.65	200	30000	15.9	$e^- p$	319
ZEUS CC	98-99	0.015	0.42	280	30000	16.4	$e^- p$	319
ZEUS NC	99-00	0.005	0.65	200	30000	63.2	$e^+ p$	319
ZEUS CC	99-00	0.008	0.42	280	17000	60.9	$e^+ p$	319

High Q^2 NC and CC data limited to
100 pb⁻¹ e^+p
16 pb⁻¹ e^-p

Up till now HERA-II datasets only partially published

ZEUS CC e ⁻ p	175 pb ⁻¹	EPJ C 61 (2009)
ZEUS CC e ⁺ p	132 pb ⁻¹	EPJ C 70 (2010)
ZEUS NC e ⁻ p	170 pb ⁻¹	EPJ C 62 (2009)
ZEUS NC e ⁺ p	135 pb ⁻¹	ZEUS-prel-11-003
H1 CC e ⁻ p	149 pb ⁻¹	H1prelim-09-043
H1 CC e ⁺ p	180 pb ⁻¹	H1prelim-09-043
H1 NC e ⁻ p	149 pb ⁻¹	H1prelim-09-042
H1 NC e ⁺ p	180 pb ⁻¹	H1prelim-09-042



ZEUS CC e ⁻ p	175 pb ⁻¹	EPJ C 61 (2009)
ZEUS CC e ⁺ p	132 pb ⁻¹	EPJ C 70 (2010)
ZEUS NC e ⁻ p	170 pb ⁻¹	EPJ C 62 (2009)
ZEUS NC e ⁺ p	135 pb ⁻¹	PRD 87 (2013) 052014
H1 CC e ⁻ p	149 pb ⁻¹	JHEP 09 (2012) 061
H1 CC e ⁺ p	180 pb ⁻¹	
H1 NC e ⁻ p	149 pb ⁻¹	
H1 NC e ⁺ p	180 pb ⁻¹	



HERA-II datasets
Combined in HERAPDF1.5
(except ZEUS NC e⁺p)

breakdown of HERA-II data samples

	<i>R</i>	<i>L</i>
<i>e⁻p</i>	$\mathcal{L} = 47.3 \text{ pb}^{-1}$ $P_e = (+36.0 \pm 1.0)\%$	$\mathcal{L} = 104.4 \text{ pb}^{-1}$ $P_e = (-25.8 \pm 0.7)\%$
<i>e⁺p</i>	$\mathcal{L} = 101.3 \text{ pb}^{-1}$ $P_e = (+32.5 \pm 0.7)\%$	$\mathcal{L} = 80.7 \text{ pb}^{-1}$ $P_e = (-37.0 \pm 0.7)\%$

Complete the analyses of HERA high Q^2
inclusive structure function data

New published data increase $\int \mathcal{L}$ by
~ factor 3 for e⁺p
~ factor 10 for e⁻p
much improved systematic uncertainties

→ HERAPDF2.0

HERA Structure Function Data



Data Set	x Grid		Q^2/GeV^2 Grid		\mathcal{L} pb^{-1}	e^+/e^-	\sqrt{s} GeV	x, Q^2 from equations	Ref.	
	from	to	from	to						
HERA I $E_p = 820 \text{ GeV}$ and $E_p = 920 \text{ GeV}$ data sets										
H1 svx-mb	95-00	0.000005	0.02	0.2	12	2.1	e^+p	301, 319	11,15,16	[2]
H1 low Q^2	96-00	0.0002	0.1	12	150	22	e^+p	301, 319	11,15,16	[3]
H1 NC	94-97	0.0032	0.65	150	30000	35.6	e^+p	301	17	[4]
H1 CC	94-97	0.013	0.40	300	15000	35.6	e^+p	301	12	[4]
H1 NC	98-99	0.0032	0.65	150	30000	16.4	e^-p	319	17	[5]
H1 CC	98-99	0.013	0.40	300	15000	16.4	e^-p	319	12	[5]
H1 NC HY	98-99	0.0013	0.01	100	800	16.4	e^-p	319	11	[6]
H1 NC	99-00	0.0013	0.65	100	30000	65.2	e^+p	319	17	[6]
H1 CC	99-00	0.013	0.40	300	15000	65.2	e^+p	319	12	[6]
ZEUS BPC	95	0.000002	0.00006	0.11	0.65	1.65	e^+p	300	11	[10]
ZEUS BPT	97	0.0000006	0.001	0.045	0.65	3.9	e^+p	300	11, 17	[11]
ZEUS SVX	95	0.000012	0.0019	0.6	17	0.2	e^+p	300	11	[12]
ZEUS NC	96-97	0.00006	0.65	2.7	30000	30.0	e^+p	300	19	[13]
ZEUS CC	94-97	0.015	0.42	280	17000	47.7	e^+p	300	12	[14]
ZEUS NC	98-99	0.005	0.65	200	30000	15.9	e^-p	318	18	[15]
ZEUS CC	98-99	0.015	0.42	280	30000	16.4	e^-p	318	12	[16]
ZEUS NC	99-00	0.005	0.65	200	30000	63.2	e^+p	318	18	[17]
ZEUS CC	99-00	0.008	0.42	280	17000	60.9	e^+p	318	12	[18]
HERA II $E_p = 920 \text{ GeV}$ data sets										
H1 NC	03-07	0.0008	0.65	60	30000	182	e^+p	319	11, 17	[7] ¹
H1 CC	03-07	0.008	0.40	300	15000	182	e^+p	319	12	[7] ¹
H1 NC	03-07	0.0008	0.65	60	50000	151.7	e^-p	319	11, 17	[7] ¹
H1 CC	03-07	0.008	0.40	300	30000	151.7	e^-p	319	12	[7] ¹
H1 NC med Q^2 ^{*y.5}	03-07	0.0000986	0.005	8.5	90	97.6	e^+p	319	11	[9]
H1 NC low Q^2 ^{*y.5}	03-07	0.000029	0.00032	2.5	12	5.9	e^+p	319	11	[9]
ZEUS NC	06-07	0.005	0.65	200	30000	135.5	e^+p	318	11,12,18	[21]
ZEUS CC	06-07	0.0078	0.42	280	30000	132	e^+p	318	12	[22]
ZEUS NC	05-06	0.005	0.65	200	30000	169.9	e^-p	318	18	[19]
ZEUS CC	04-06	0.015	0.65	280	30000	175	e^-p	318	12	[20]
ZEUS NC nominal ^{*y}	06-07	0.000092	0.008343	7	110	44.5	e^+p	318	11	[23]
ZEUS NC satellite ^{*y}	06-07	0.000071	0.008343	5	110	44.5	e^+p	318	11	[23]
HERA II $E_p = 575 \text{ GeV}$ data sets										
H1 NC high Q^2	07	0.00065	0.65	35	800	5.4	e^+p	252	11, 17	[8]
H1 NC low Q^2	07	0.0000279	0.0148	1.5	90	5.9	e^+p	252	11	[9]
ZEUS NC nominal	07	0.000147	0.013349	7	110	7.1	e^+p	251	11	[23]
ZEUS NC satellite	07	0.000125	0.013349	5	110	7.1	e^+p	251	11	[23]
HERA II $E_p = 460 \text{ GeV}$ data sets										
H1 NC high Q^2	07	0.00081	0.65	35	800	11.8	e^+p	225	11, 17	[8]
H1 NC low Q^2	07	0.0000348	0.0148	1.5	90	12.2	e^+p	225	11	[9]
ZEUS NC nominal	07	0.000184	0.016686	7	110	13.9	e^+p	225	11	[23]
ZEUS NC satellite	07	0.000143	0.016686	5	110	13.9	e^+p	225	11	[23]

H1 & ZEUS have now published all datasets

- HERA-II measurements at high $\int \mathcal{L}$
- reduced \sqrt{s} data

41 data sets to be combined:

- NC & CC cross sections
- e^+p and e^-p scattering
- 4 different \sqrt{s} values

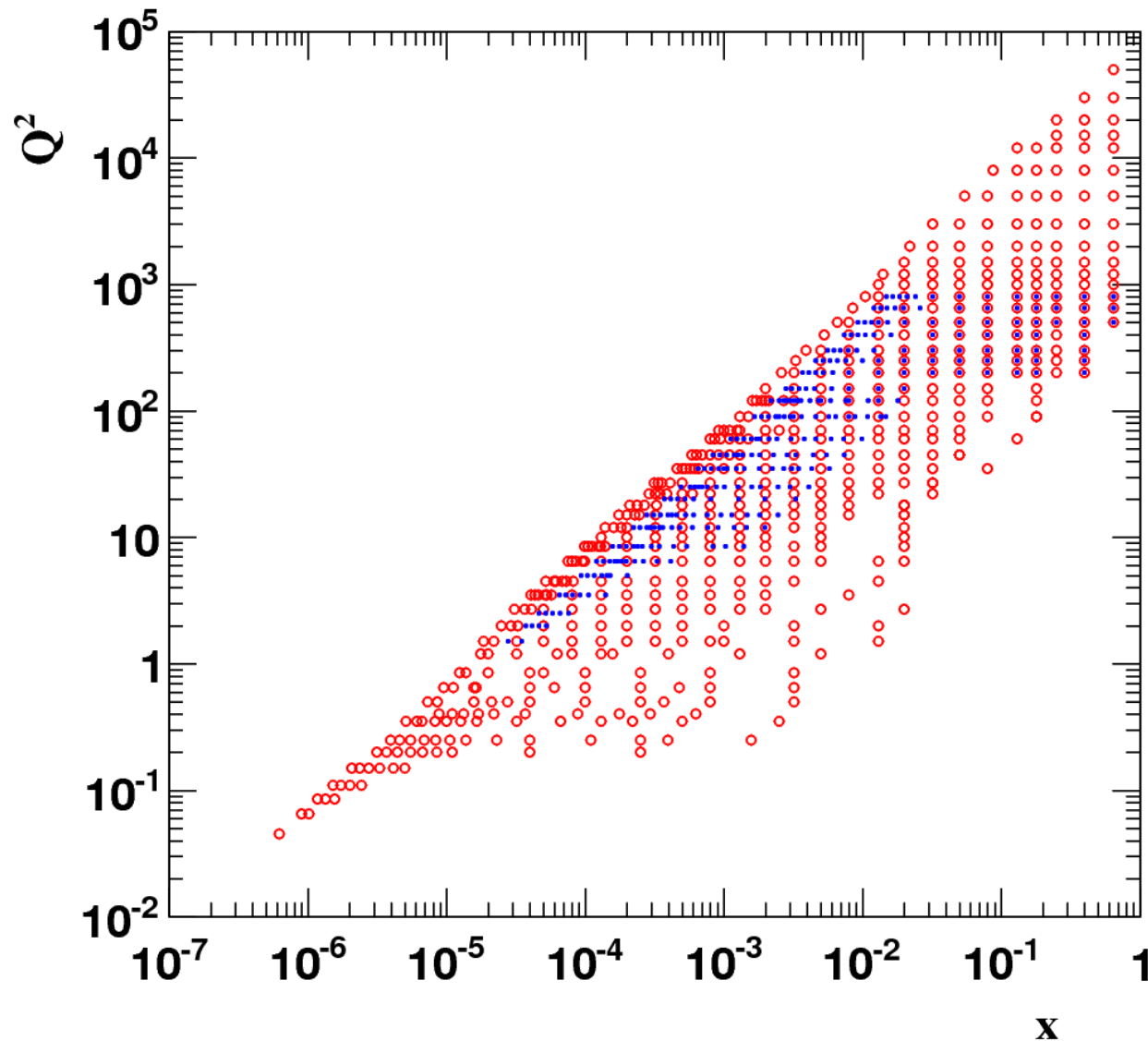
2927 data points in total \rightarrow 1307

In some cases 6 measurements combined

$$0.045 < Q^2 < 50,000 \text{ GeV}^2$$

$$6 \times 10^{-7} < x < 0.65$$

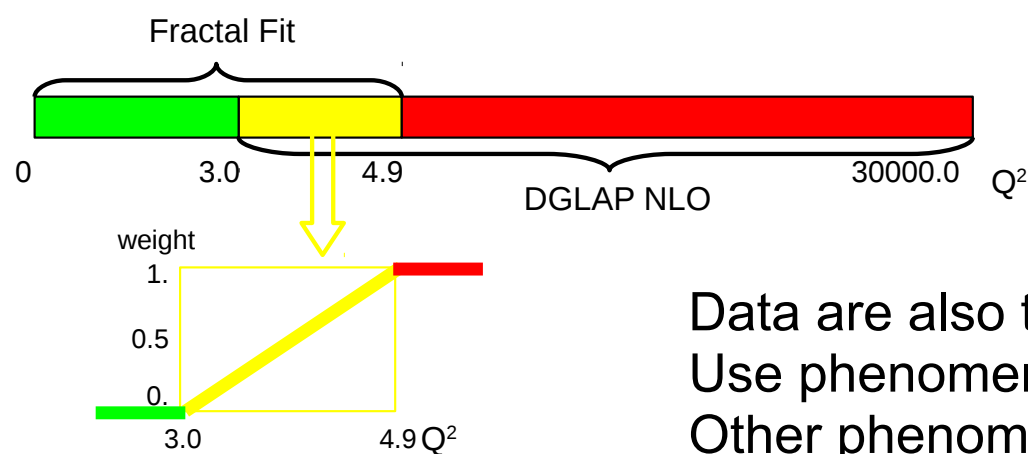
arXiv:1506.06042



Data are combined onto a common x, Q^2 grid
 Two grids used:
 inclusive measurements $\sqrt{s}=318$ GeV
 fine x grid for $\sqrt{s}=251$ & 225 GeV

2927 data points \rightarrow 1307 combined measurements

Data are translated to nearest x, Q^2 grid point
 Iterative process using NLO QCD fit to data
 Use uncombined data in first iteration
 Then combined data in later iterations
 No changes after 3 iterations



$$\sigma(x_{grid}, Q_{grid}^2) = \frac{\sigma_{model}(x_{grid}, Q_{grid}^2)}{\sigma_{model}(x_{meas}, Q_{meas}^2)} \cdot \sigma_{meas}(x_{meas}, Q_{meas}^2)$$

Data are also translated outside of region of DGLAP fit validity $Q^2 < 3.0$ GeV²
 Use phenomenological “fractal” model and interpolate to DGLAP region
 Other phenomenological fits tested \rightarrow negligible differences



i data points
 j systematic error sources

Correlated uncertainties treated multiplicative: size proportional to central averaged value
 True for normalisation uncertainties
 Perhaps not true for other uncertainties

$$\chi_{tot}^2(\mathbf{m}, \mathbf{b}) = \sum_i \frac{[\mu^i - m^i(1 - \sum_j \gamma_j^i b_j)]^2}{\delta_{i,stat}^2 \mu^i m^i (1 - \sum_j \gamma_j^i b_j) + (\delta_{i,unc} m^i)^2} + \sum_j b_j^2$$

μ^i = measurement

m^i = averaged value

γ_j^i = correlated relative (%) sys uncertainty on point i from error source j

b_j = systematic error source strength

nuisance parameter left free in fit but constrained
 no extra degrees of freedom due to additional constraint

For HERAPDF2.0 number of correlated error sources $j = 169$

These include:

- b/g uncertainty
- luminosity uncertainty
- EM calibration scale
- had calibration scale
- etc....

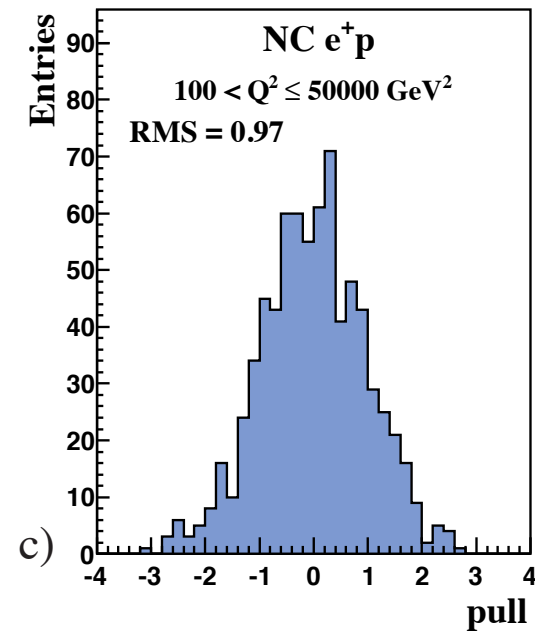
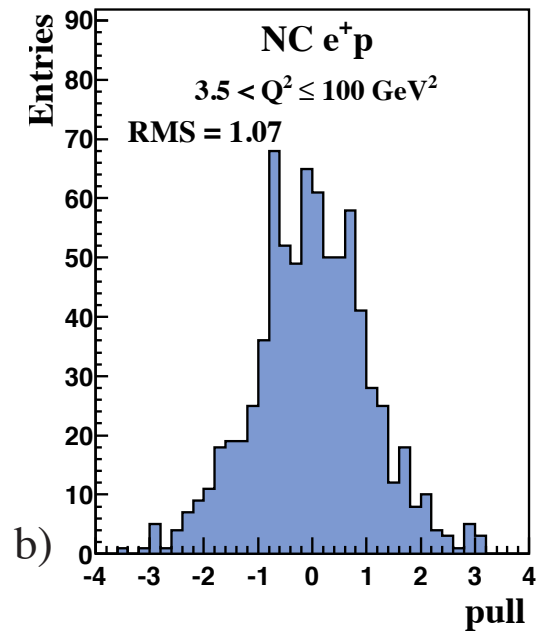
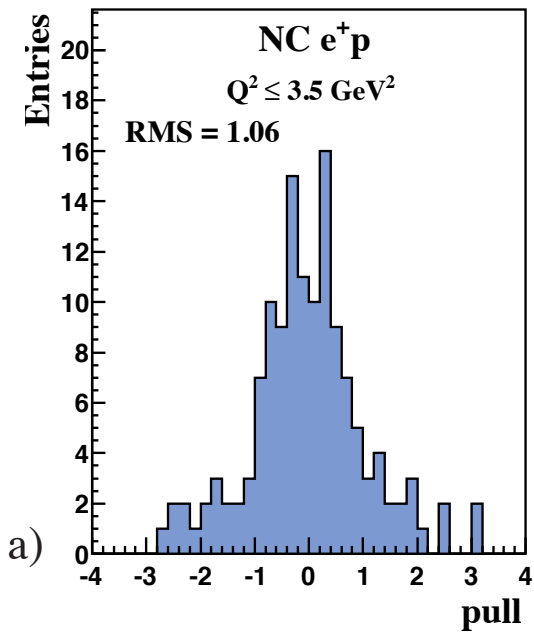
Extra procedural uncertainty included:
 difference between using
 additive vs multiplicative
 correlated uncertainties (except normalisation)
 ⇒ extra ~0.5% uncertainty

Are correlated point-to-point within a single measurement

Reported in detail in individual publications from experiments

May also be correlated across measurements

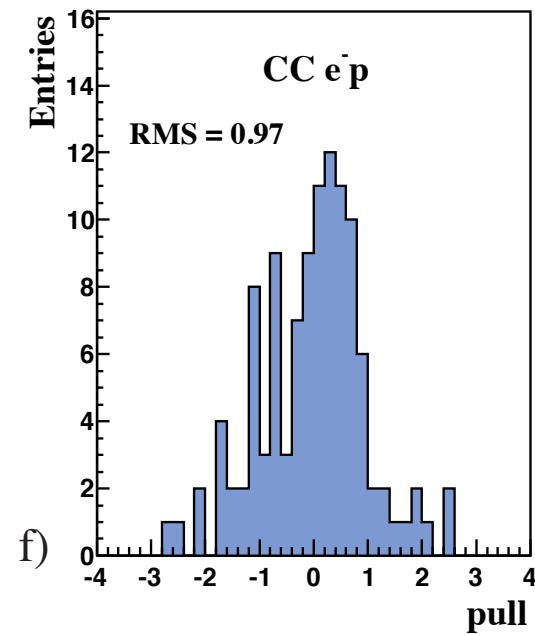
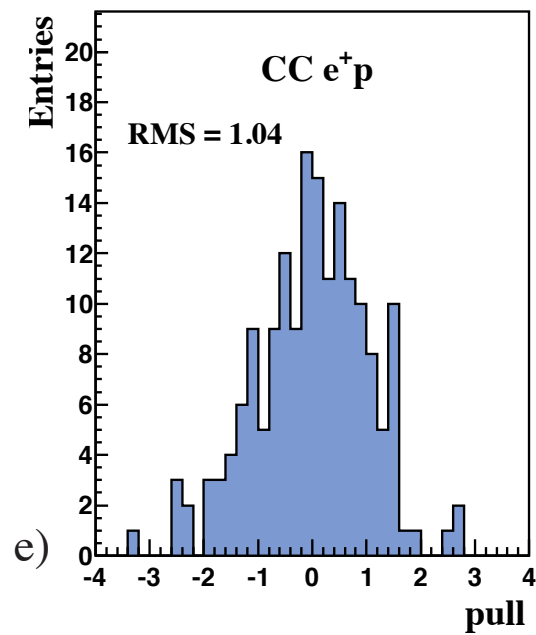
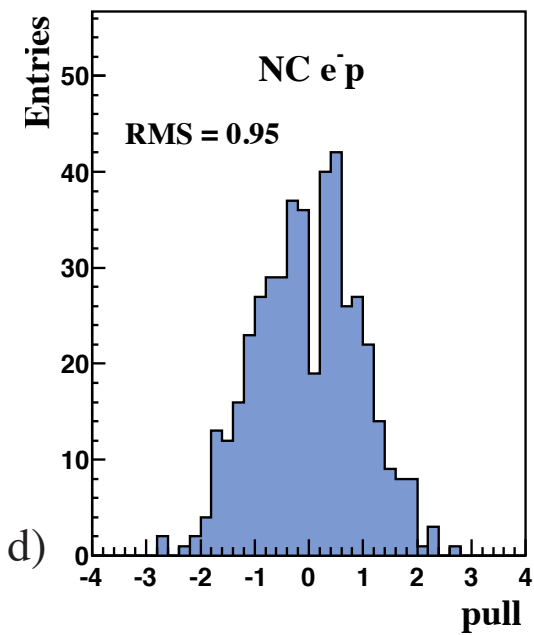
May also be correlated between H1 & ZEUS (e.g. had scale & photo-production b/g)



Overall $\chi^2/\text{ndf} = 1685 / 1620 = 1.04$

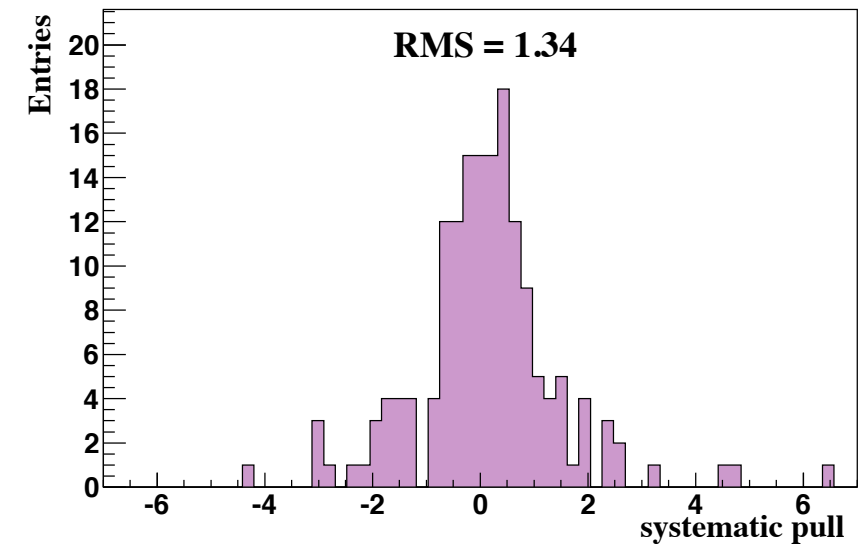
Pulls defined for each measurement difference between measured & average values after applying sys shifts b_j in units of uncorrelated uncertainty

Pulls of the data points should be distributed as a unit Gaussian

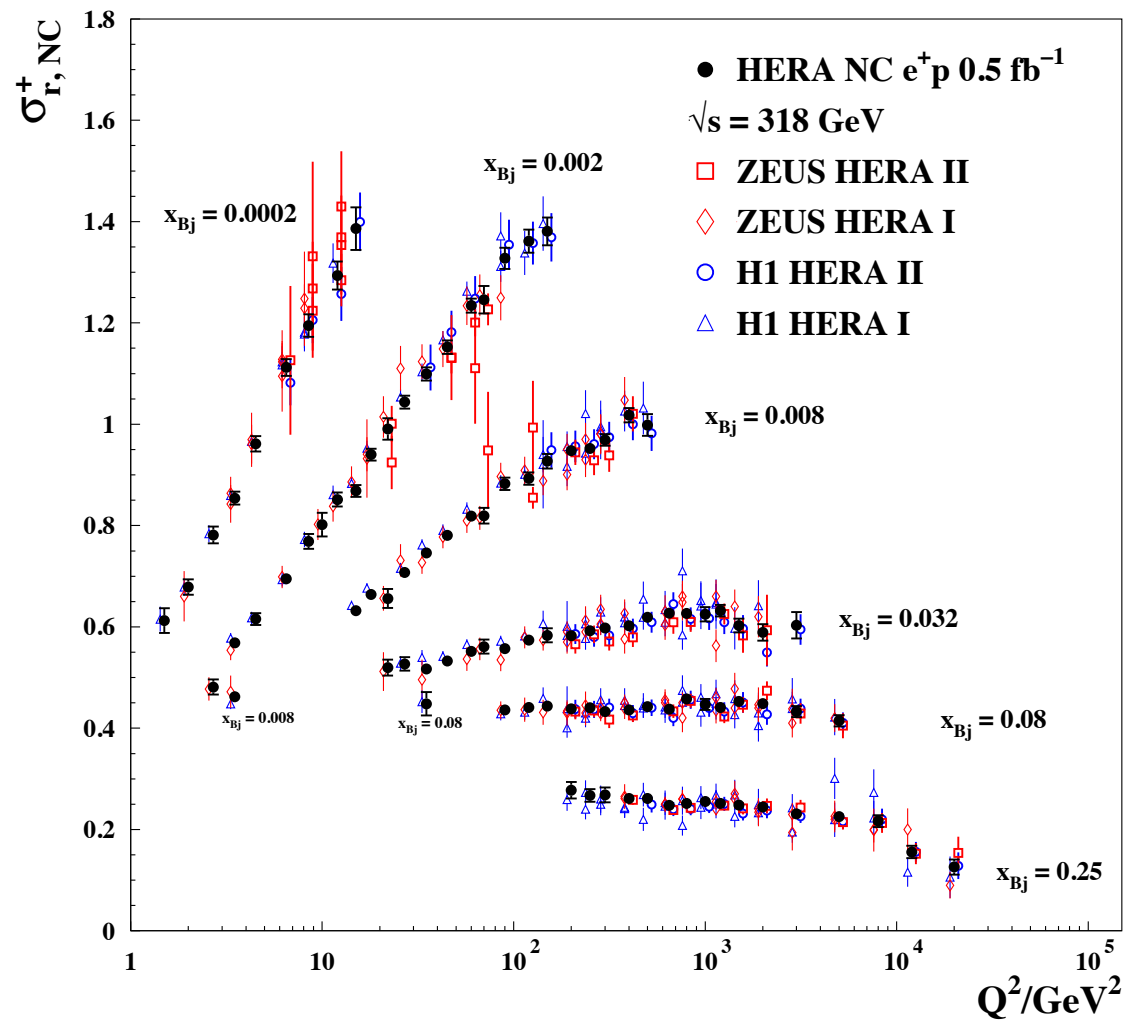


Each measurement channel shows pull centred on zero & unit width

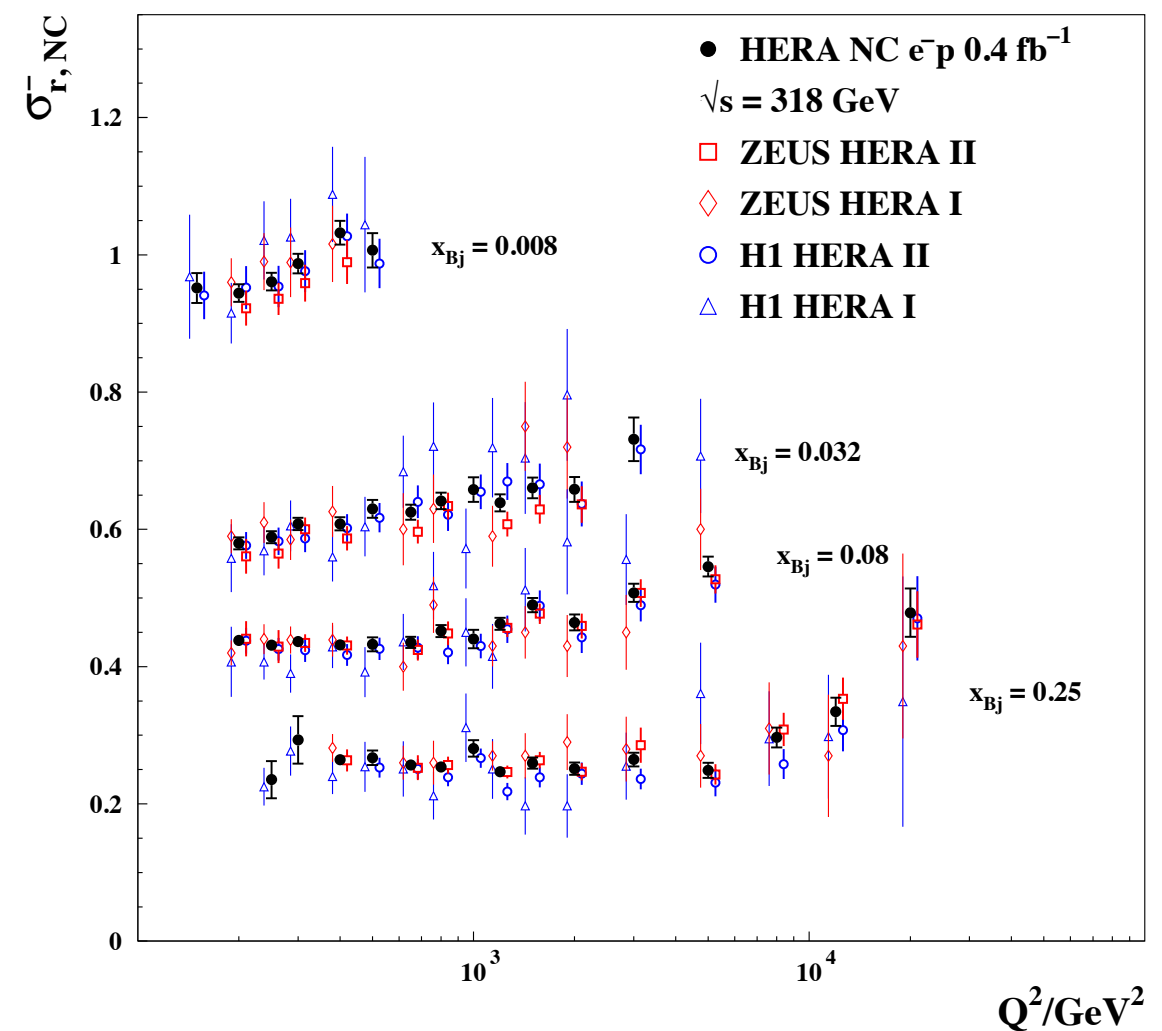
pulls of the systematic sources b_j



e^+p



e^-p



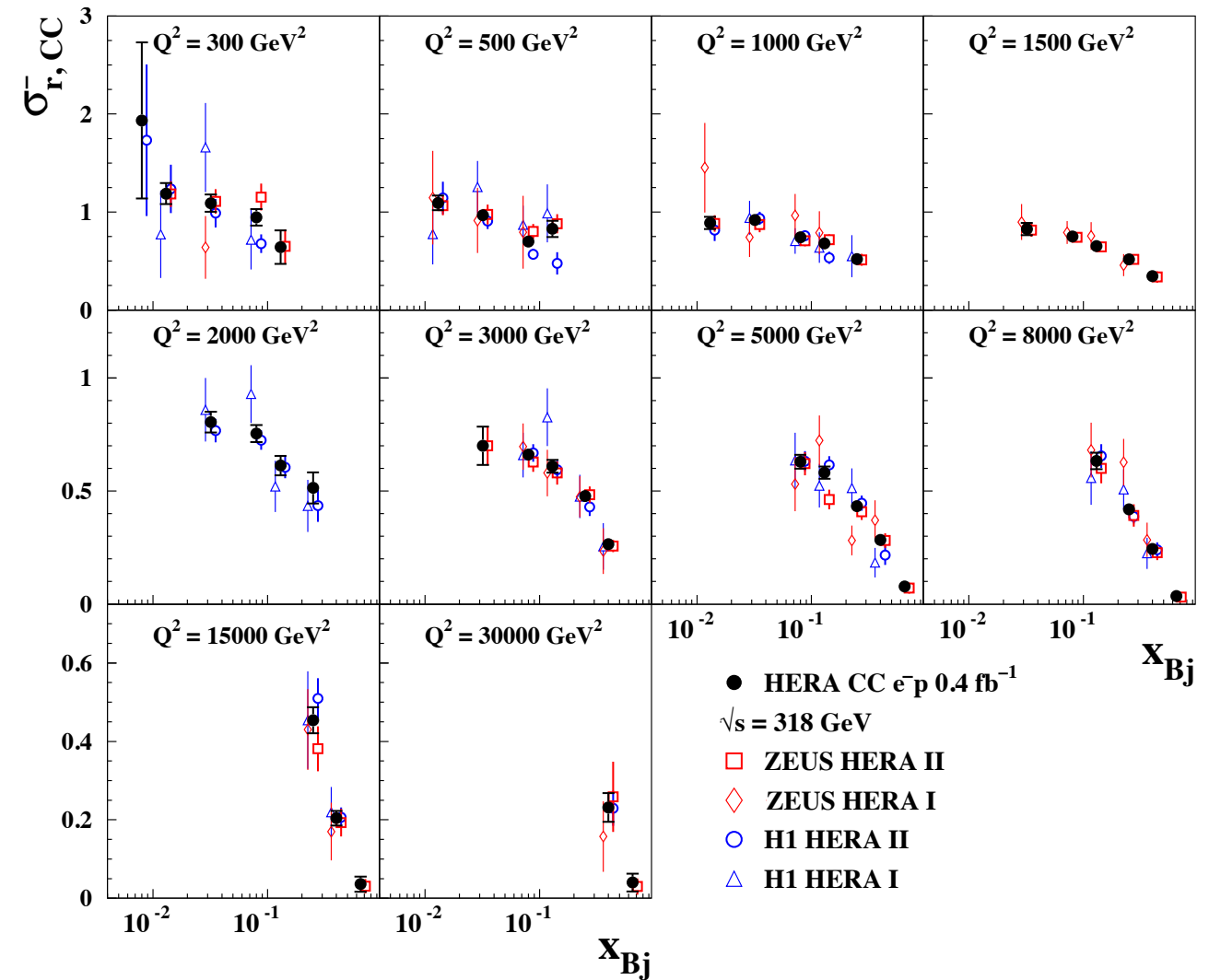
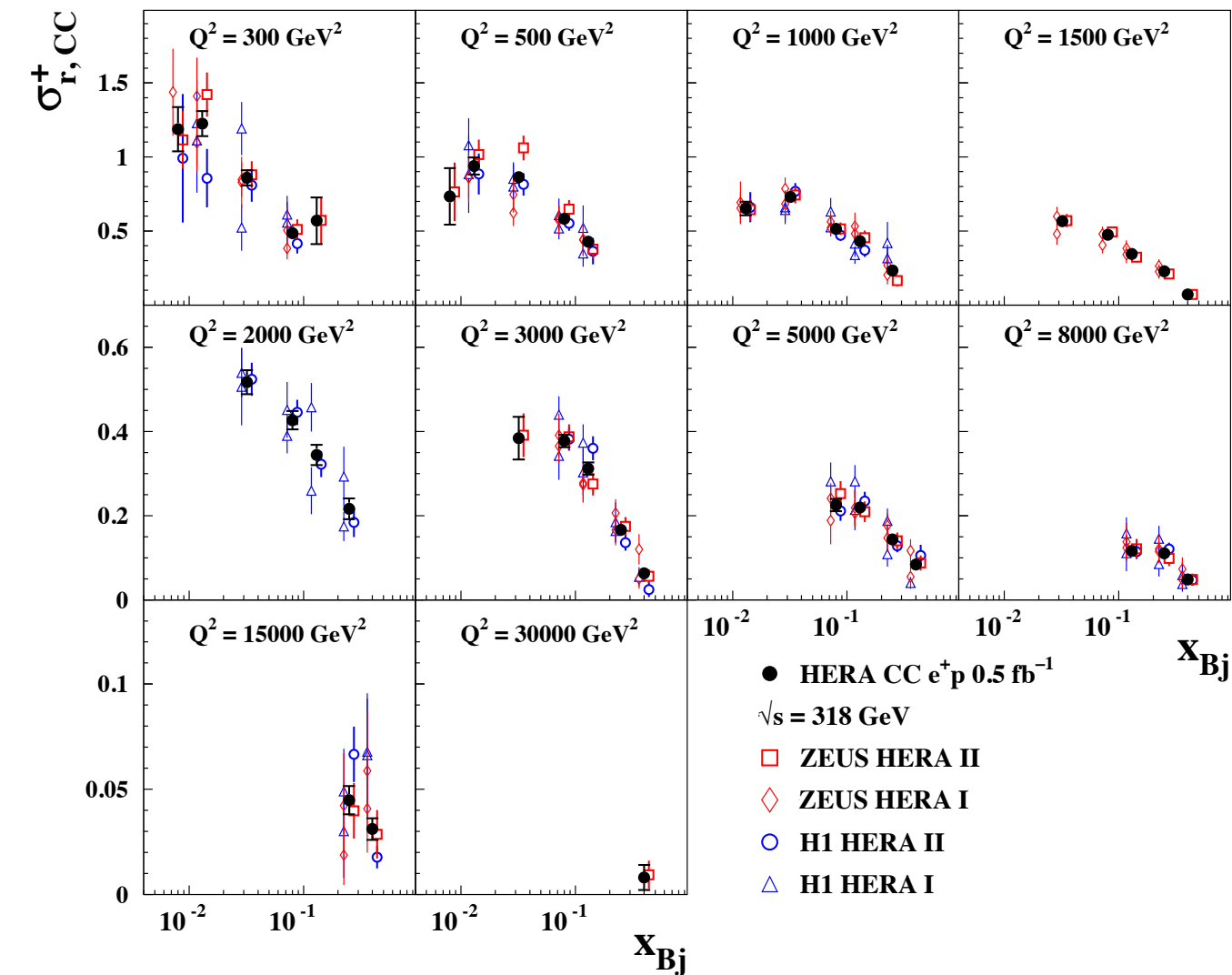
only 6 x bins shown here
 factor 10 more data than HERA-I data sets
 NC e^+p data systematically limited

$$\chi^2 / \text{ndf} = 1687 / 1620$$

high precision reached over large kinematic range better than 1.3% $Q^2 < 400 \text{ GeV}^2$

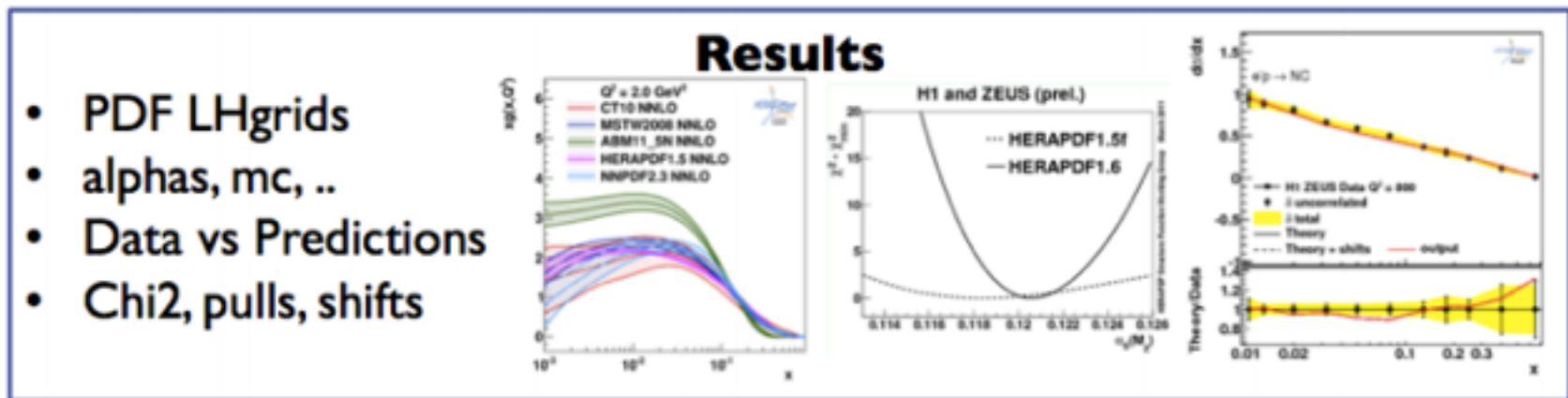
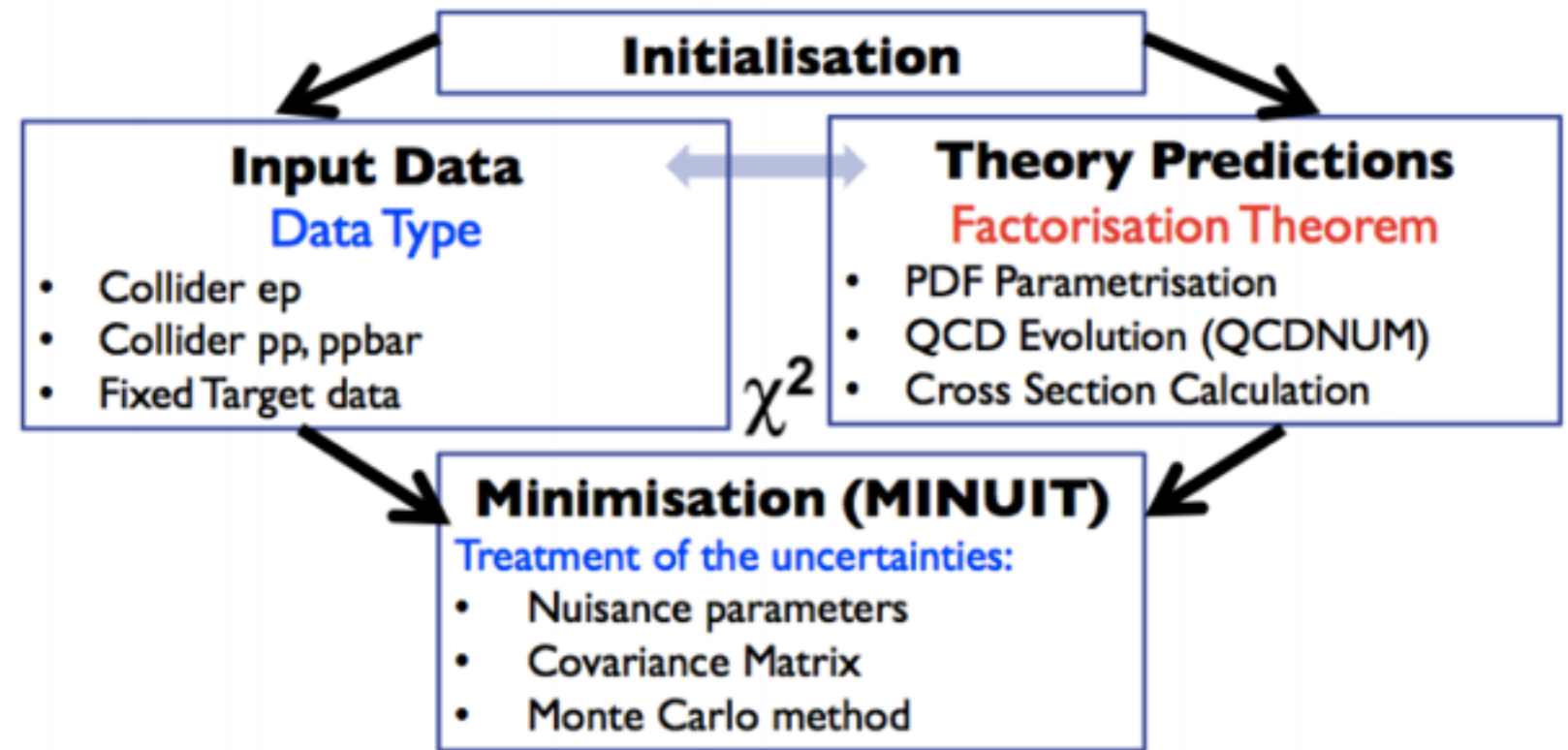
e^+p

e^-p



Large improvement in statistical limitations of individual data sets from H1 & ZEUS

- Parameterise PDFs at arbitrary starting scale Q_0^2
- Perturbative QCD evolution equations allows PDFs to be determined at any other scale Q^2
- Calculate theory cross section at given x, Q^2 of measurement
- Compare data & theory via χ^2 function
- Minimise χ^2 function with respect to PDF parameters ~ 2000 iterations





HERAPDF1.0 & 1.5

Combine NC and CC HERA-I data from H1 & ZEUS
 Complete MSbar NLO fit
 NLO: standard parameterisation with 10 parameters
 NNLO HERAPDF 1.5 with 14p

HERAPDF2.0

Include additional NC and CC HERA-II combined data
 Complete MSbar NLO and NNLO fit
 NLO & NNLO fits require 15 parameters

$$xf(x, Q_0^2) = A \cdot x^B \cdot (1-x)^C \cdot (1 + Dx + Ex^2)$$

xg	xg	$xg(x) = A_g x^{B_g} (1-x)^{C_g}$	$xg(x) = A_g x^{B_g} (1-x)^{C_g} - A'_g x^{B'_g} (1-x)^{C'_g}$
xu_v	$xU = xu + xc$	$xu_v(x) = A_{u_v} x^{B_{u_v}} (1-x)^{C_{u_v}} (1 + E_{u_v} x^2)$	$xu_v(x) = A_{u_v} x^{B_{u_v}} (1-x)^{C_{u_v}} (1 + E_{u_v} x^2)$
xd_v	$xD = xd + xs$	$xd_v(x) = A_{d_v} x^{B_{d_v}} (1-x)^{C_{d_v}}$	$xd_v(x) = A_{d_v} x^{B_{d_v}} (1-x)^{C_{d_v}}$
$x\bar{U}$	$x\bar{U} = x\bar{u} + x\bar{c}$	$x\bar{U}(x) = A_{\bar{U}} x^{B_{\bar{U}}} (1-x)^{C_{\bar{U}}}$	$x\bar{U}(x) = A_{\bar{U}} x^{B_{\bar{U}}} (1-x)^{C_{\bar{U}}} (1 + D_{\bar{U}} x)$
$x\bar{D}$	$x\bar{D} = x\bar{d} + x\bar{s}$	$x\bar{D}(x) = A_{\bar{D}} x^{B_{\bar{D}}} (1-x)^{C_{\bar{D}}}$	$x\bar{D}(x) = A_{\bar{D}} x^{B_{\bar{D}}} (1-x)^{C_{\bar{D}}}$

HERAPDF1.0 & NLO HERAPDF1.5

HERAPDF2.0

$x\bar{s} = f_s x\bar{D}$ strange sea is a fixed fraction f_s of D at Q_0^2

Apply momentum/counting sum rules:

$$\int_0^1 dx \cdot (xu_v + xd_v + x\bar{U} + x\bar{D} + xg) = 1$$

$$\int_0^1 dx \cdot u_v = 2 \quad \int_0^1 dx \cdot d_v = 1$$

$$B_{\bar{U}} = B_{\bar{D}}$$

$$Sea = 2(\bar{U} + \bar{D})$$

$$A_{\bar{U}} = A_{\bar{D}}(1 - f_s)$$

ensures $x\bar{u} \rightarrow x\bar{d}$ as $x \rightarrow 0$

$$Q_0^2 = 1.9$$

$$Q_{\min}^2 = 3.5 \text{ or } 10 \text{ GeV}^2$$

$$\alpha_s(M_z^2) = 0.118$$

$$2 \cdot 10^{-4} \leq x \leq 0.65$$

$$\begin{aligned}
 xg(x) &= A_g x^{B_g} (1-x)^{C_g} - A'_g x^{B'_g} (1-x)^{C'_g}, \\
 xu_v(x) &= A_{u_v} x^{B_{u_v}} (1-x)^{C_{u_v}} (1 + E_{u_v} x^2), \\
 xd_v(x) &= A_{d_v} x^{B_{d_v}} (1-x)^{C_{d_v}}, \\
 x\bar{U}(x) &= A_{\bar{U}} x^{B_{\bar{U}}} (1-x)^{C_{\bar{U}}} (1 + D_{\bar{U}} x), \\
 x\bar{D}(x) &= A_{\bar{D}} x^{B_{\bar{D}}} (1-x)^{C_{\bar{D}}}.
 \end{aligned}$$

■ fixed or constrained by sum-rules

■ parameters set equal but free

NC structure functions

$$\begin{aligned}
 F_2 &= \frac{4}{9} (xU + x\bar{U}) + \frac{1}{9} (xD + x\bar{D}) \\
 xF_3 &\sim xu_v + xd_v
 \end{aligned}$$

CC structure functions

$$\begin{aligned}
 W_2^- &= x(U + \bar{D}), & W_2^+ &= x(\bar{U} + D) \\
 xW_3^- &= x(U - \bar{D}), & xW_3^+ &= x(D - \bar{U})
 \end{aligned}$$

Additional parameters:

heavy quark masses M_c and M_b are optimised

$f_s = 0.4 \Rightarrow$ compromise value between unsuppressed ($f_s = 0.5$) and 'default' strange sea from dimuon data

$$\chi_{tot}^2(\mathbf{m}, \mathbf{b}) = \sum_i \frac{[\mu^i - m^i(1 - \sum_j \gamma_j^i b_j)]^2}{\delta_{i,stat}^2 \mu^i m^i (1 - \sum_j \gamma_j^i b_j) + (\delta_{i,unc} m^i)^2} + \sum_j b_j^2 + \sum_i \ln \frac{\delta_{i,unc}^2 m_i^2 + \delta_{i,stat}^2 \mu^i m^i}{\delta_{i,unc}^2 \mu_i^2 + \delta_{i,stat}^2 \mu_i^2}$$

modified χ^2 definition includes ln term to account for likelihood transition to χ^2 after error scaling

Experimental Uncertainties

Hessian method uses 14 eigenvector pairs
Standard definition $\Delta\chi^2=1$ for 68% CL error bands

Model Assumptions

Variation of charm and bottom quark masses M_c , M_b
Variation of Q^2 minimum cut used on input data Q_{\min}^2
Variation of strange quark fraction f_s

Parameterisation Uncertainties

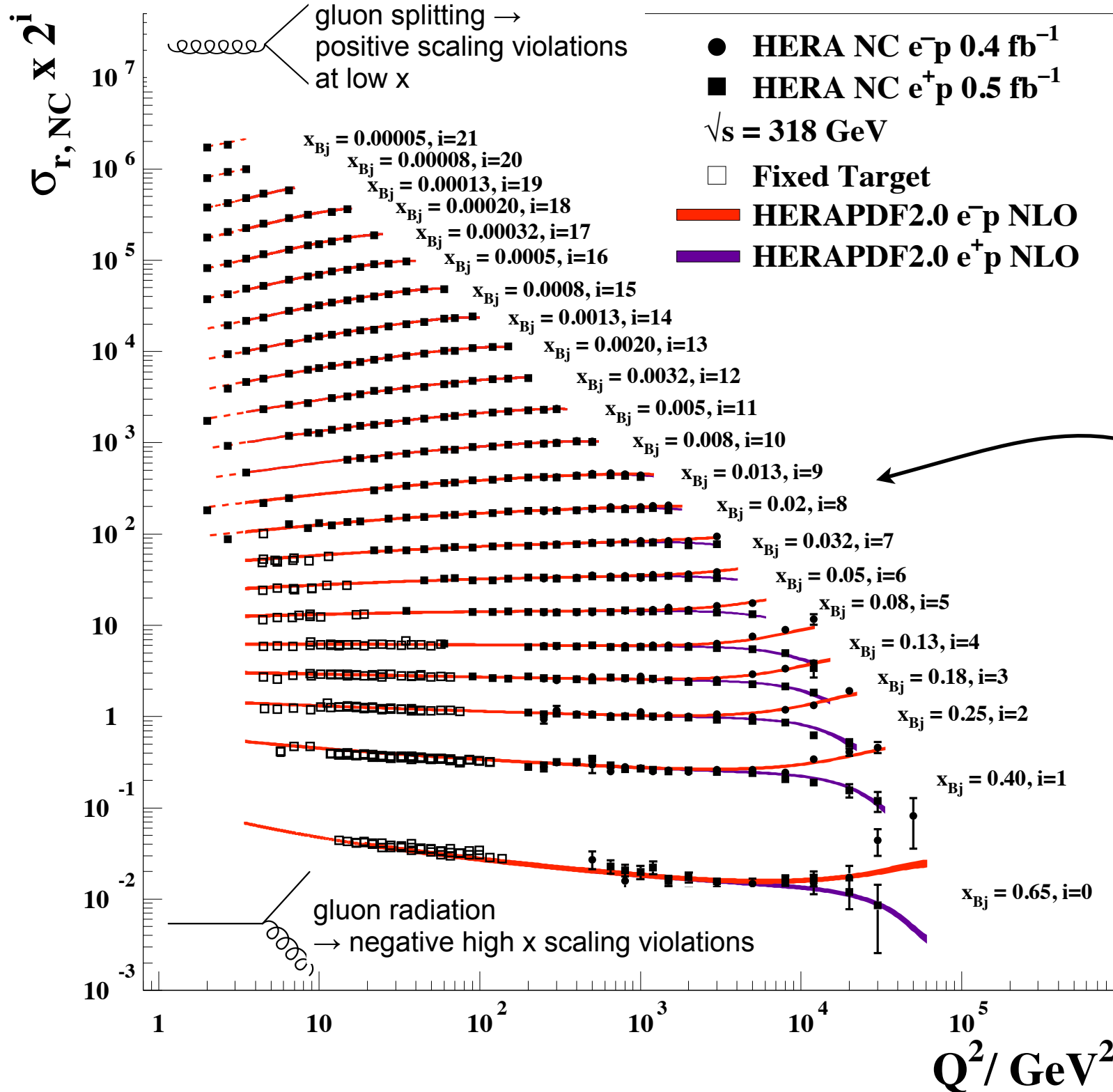
Variation of Q_0^2
Variation of fit using additional 15th parameter

Variation	Standard Value	Lower Limit	Upper Limit
Q_{\min}^2 [GeV ²]	3.5	2.5	5.0
Q_{\min}^2 [GeV ²] HiQ2	10.0	7.5	12.5
M_c (NLO) [GeV]	1.47	1.41	1.53
M_c (NNLO) [GeV]	1.43	1.37	1.49
M_b [GeV]	4.5	4.25	4.75
f_s	0.4	0.3	0.5
$\alpha_s(M_Z^2)$	0.118	–	–
μ_{f_0} [GeV]	1.9	1.6	2.2

$\alpha_s(M_Z^2)$ is fixed but series of PDFs provided scanning large range in value: 0.110 to 0.130

Experimental uncertainties also checked using RMS spread of 400 replica fits

Neutral Current $e^\pm p$



Precision 1.3% for $Q^2 < 400 \text{ GeV}^2$
 \Rightarrow factor 2 reduction in error wrt HERA-I

Statistics limited at higher Q^2 and high x

Extended reach at high x compared to H1 preliminary data

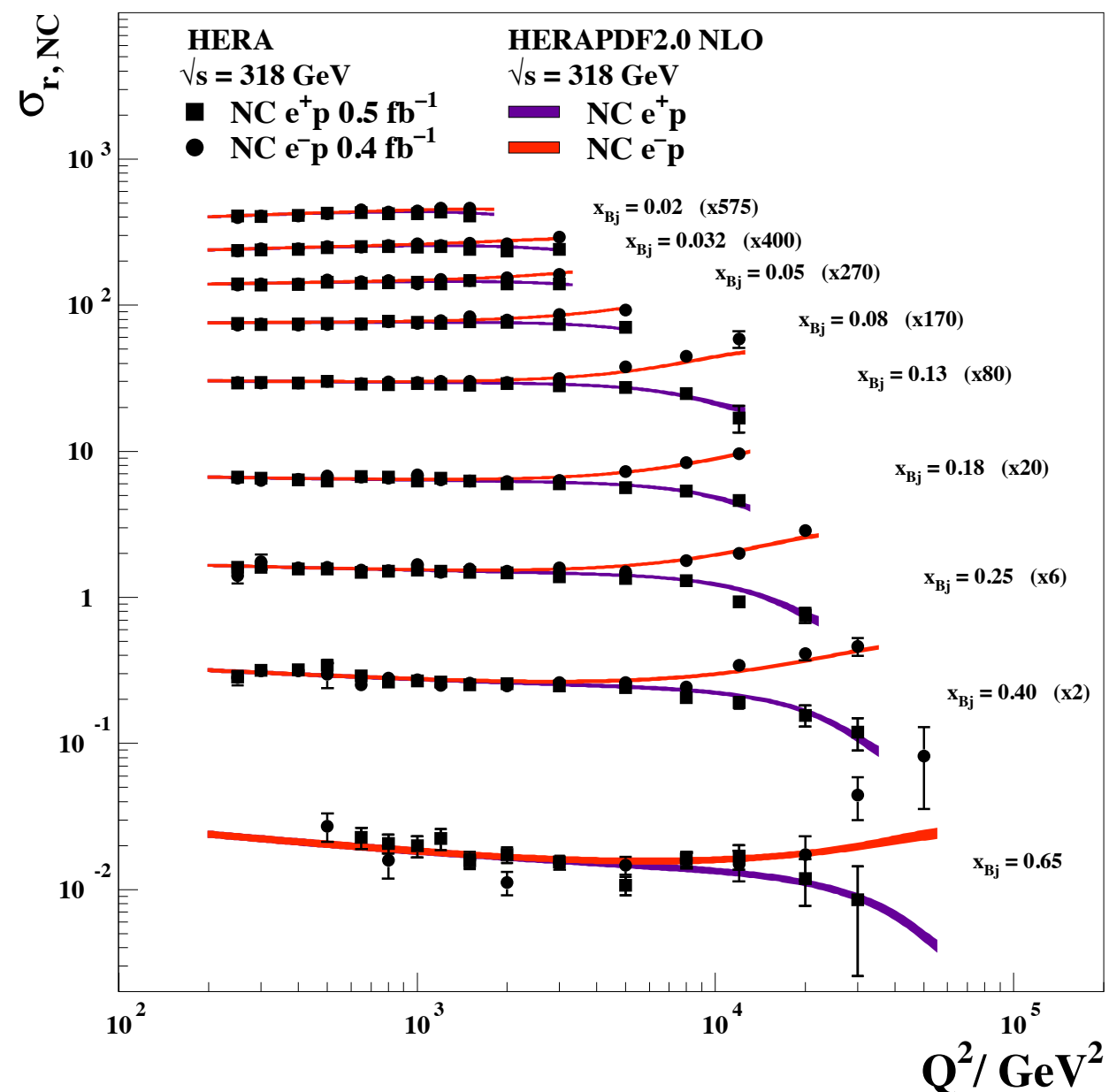
This x region is the 'sweet spot'
 High precision with long Q^2 lever arm
 x -range relevant for Higgs production

Combination of high Q^2 data
 HERA-1 and HERA-II

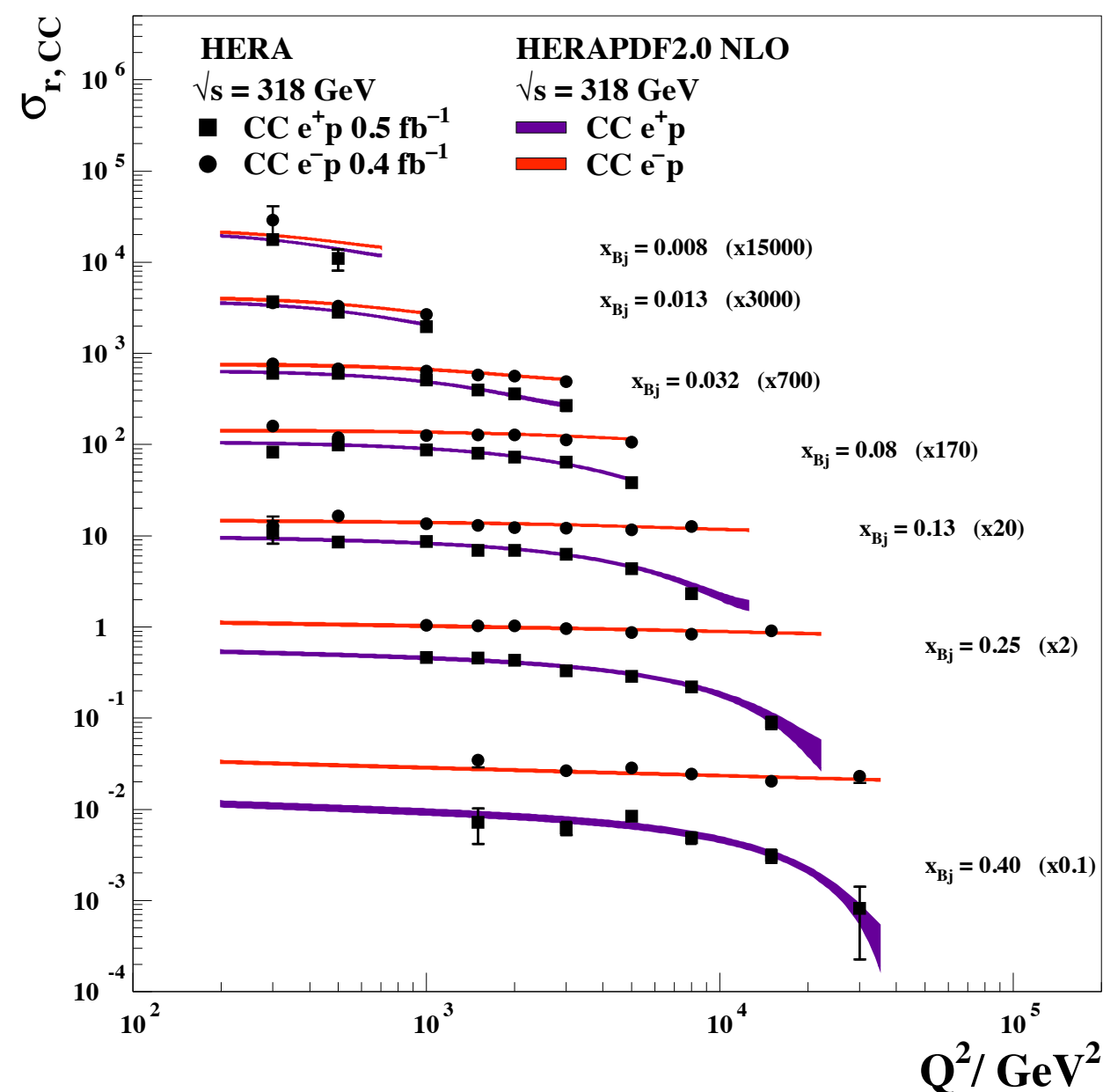
Larger HERA-II luminosity
 \rightarrow improved precision at high x / Q^2

HERAPDF2.0 provides good description

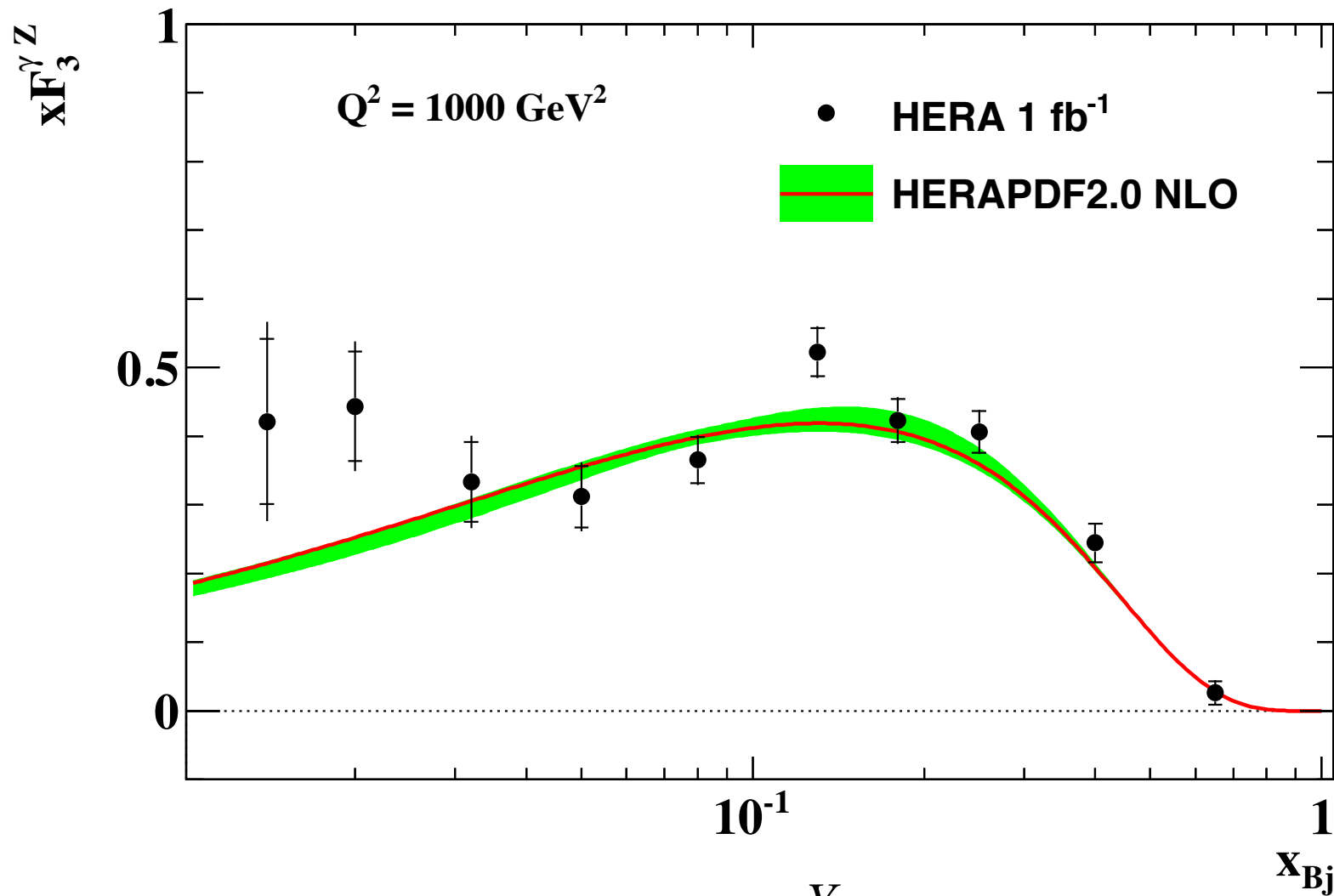
Neutral Current $e^\pm p$



Charged Current $e^\pm p$



- Difference in NC at high x for e^+ and e^- is due to xF_3 and Z boson exchange \rightarrow valence quarks
- CC e^+p suppressed at high x due to $(1-y)^2$ helicity suppression of quarks at high y, Q^2 & fixed x
- CC e^-p unaffected as helicity suppression applies to anti-quarks
- HERAPDF2.0 describes high x data well for both NC and CC channels



At high Q^2 xF_3 arises due to Z^0 effects
 enhanced e^- cross section wrt e^+
 Difference is xF_3
 Sensitive to valence PDFs

$$x\tilde{F}_3 = \frac{Y_+}{2Y_-} (\tilde{\sigma}_{NC}^- - \tilde{\sigma}_{NC}^+) \approx a_e \chi_Z xF_3^{\gamma Z}$$

$$x\tilde{F}_3 \propto \sum (xq_i - x\bar{q}_i)$$

Measure integral of $xF_3^{\gamma Z}$ - validate sumrule:

$$\int_{0.016}^{0.725} dx F_3^{\gamma Z}(x, Q^2 = 1500 \text{ GeV}^2) = 1.314 \pm 0.057(\text{stat}) \pm 0.057(\text{syst})$$

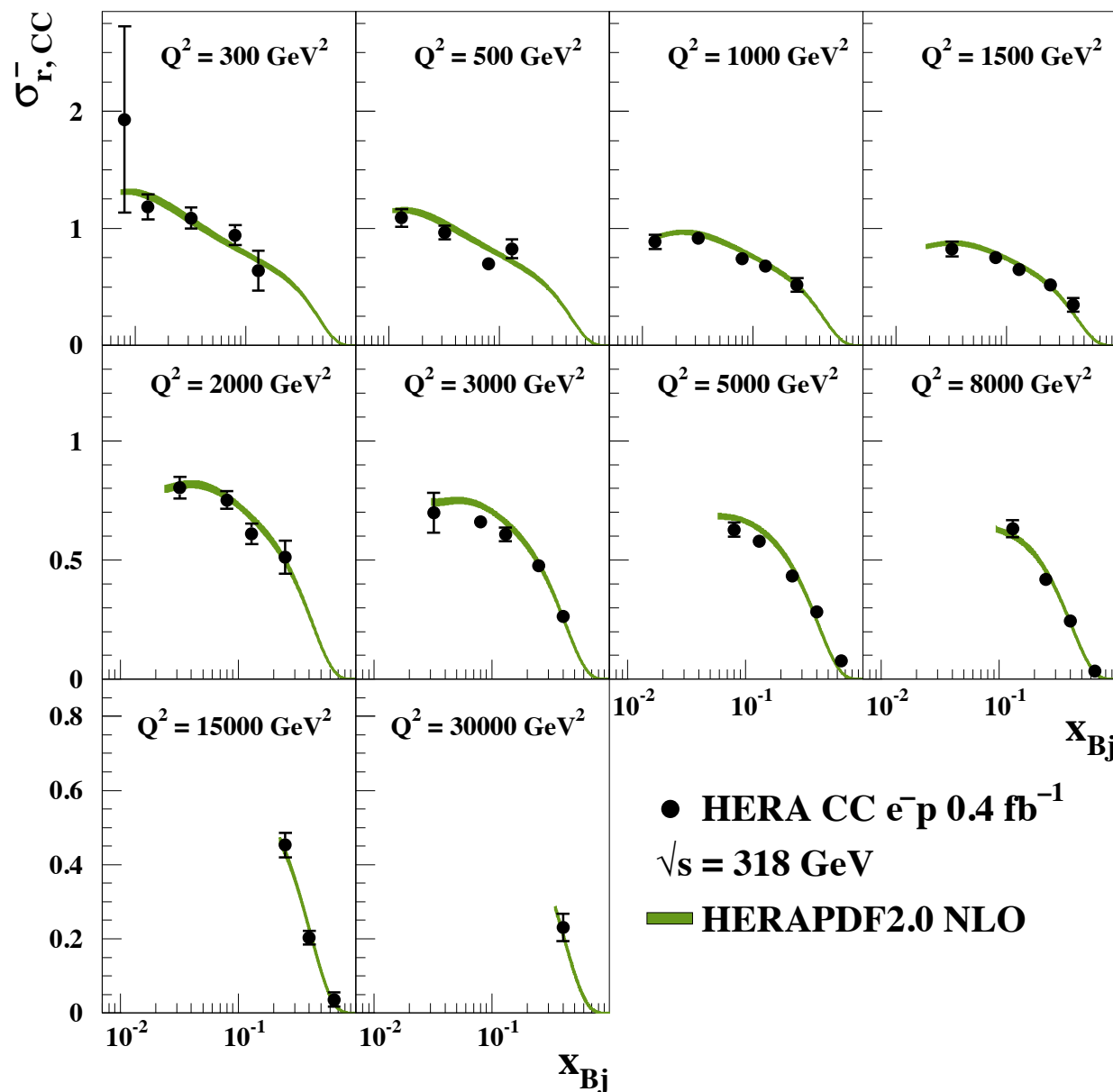
LO integral predicted to
 be $5/3 + \mathcal{O}(\alpha_s/\pi)$

Electron scattering

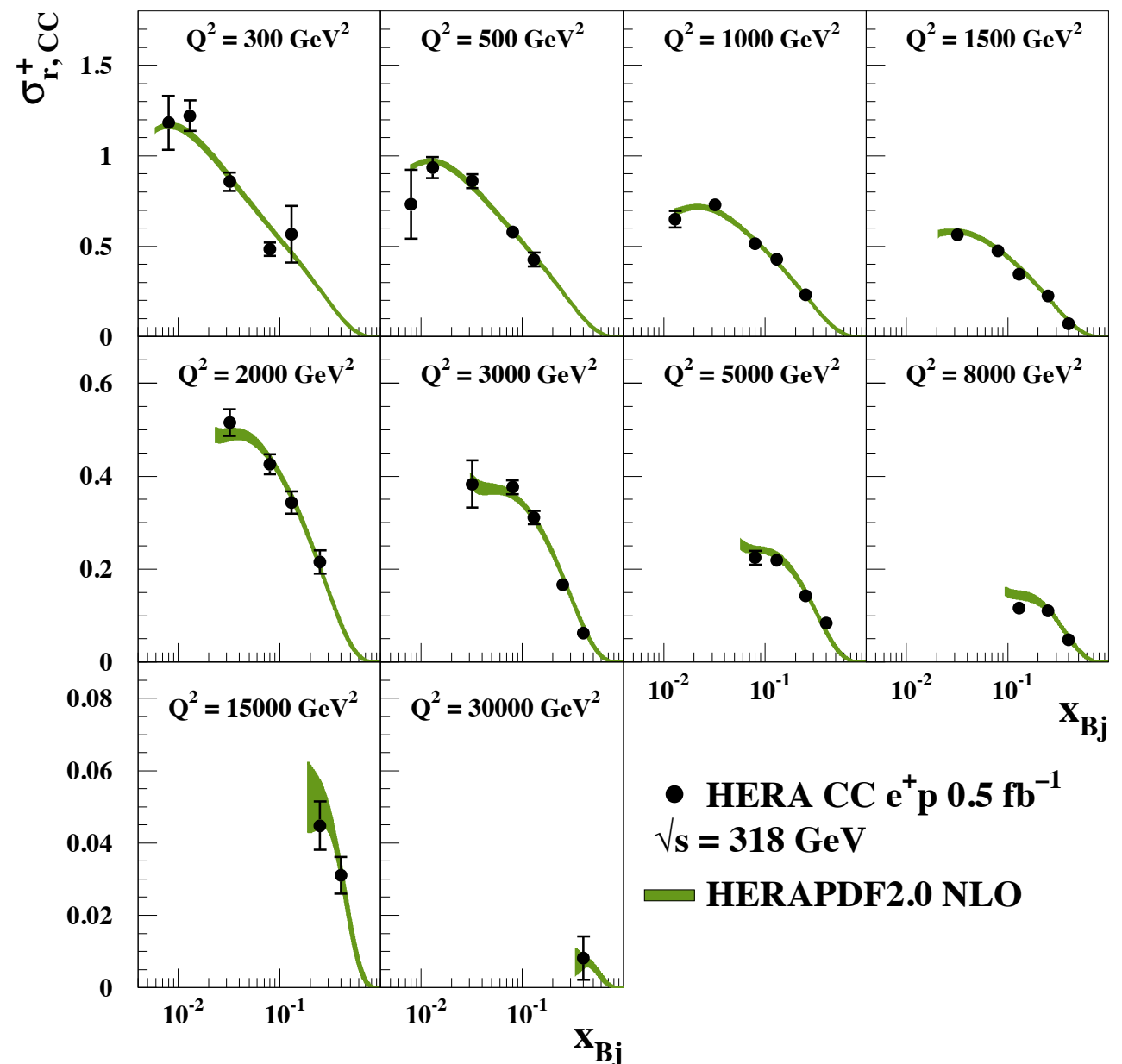
$$\frac{d^2\sigma_{CC}^-}{dx dQ^2} = \frac{G_F^2}{2\pi} \left(\frac{M_W^2}{M_W^2 + Q^2} \right)^2 \left[(u + c) + (1 - y)^2 (\bar{d} + \bar{s}) \right]$$

Positron scattering

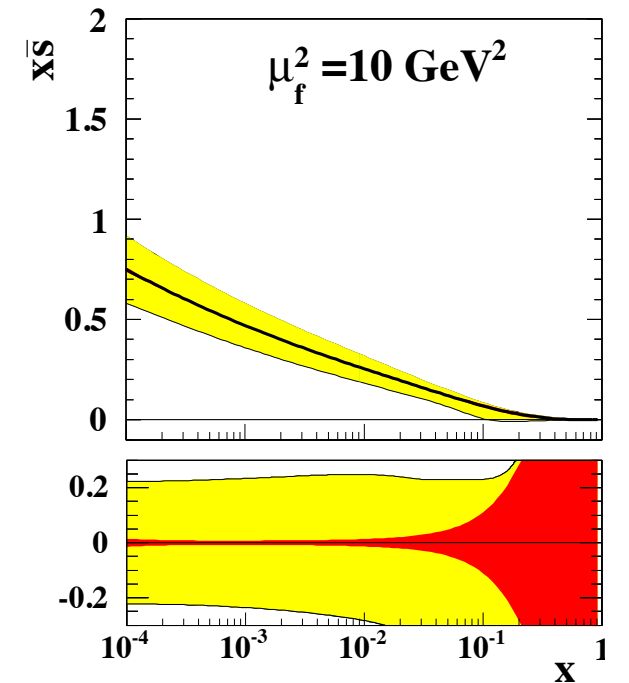
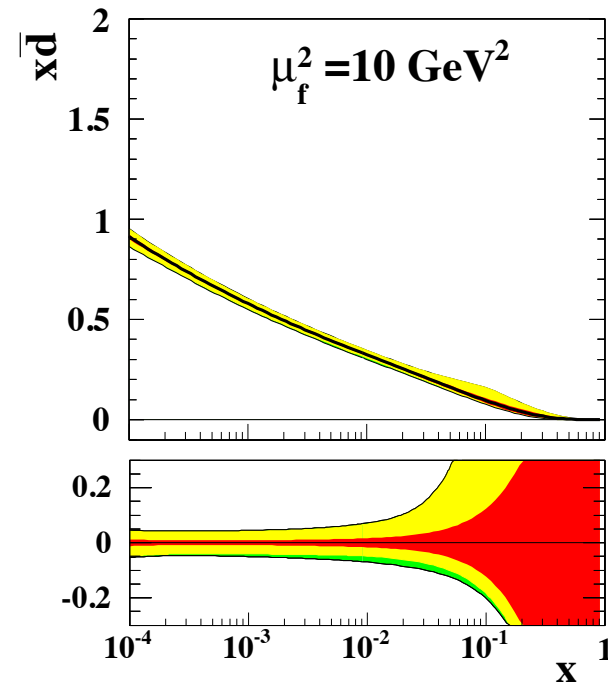
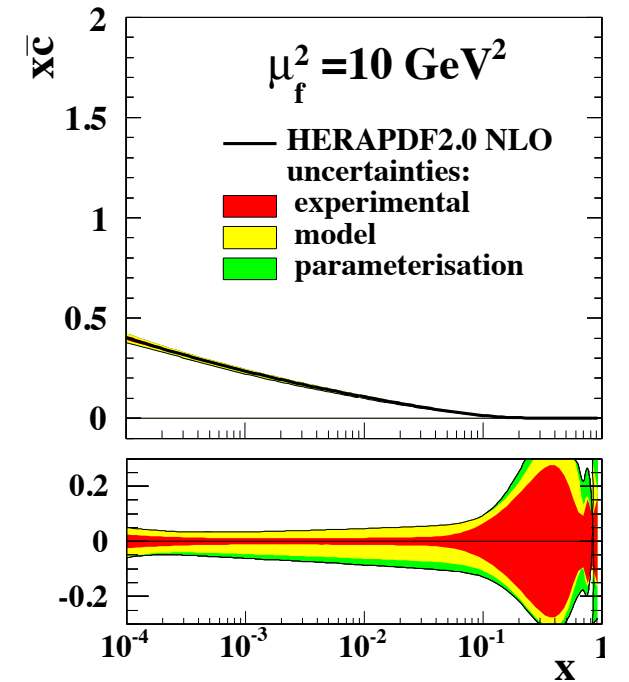
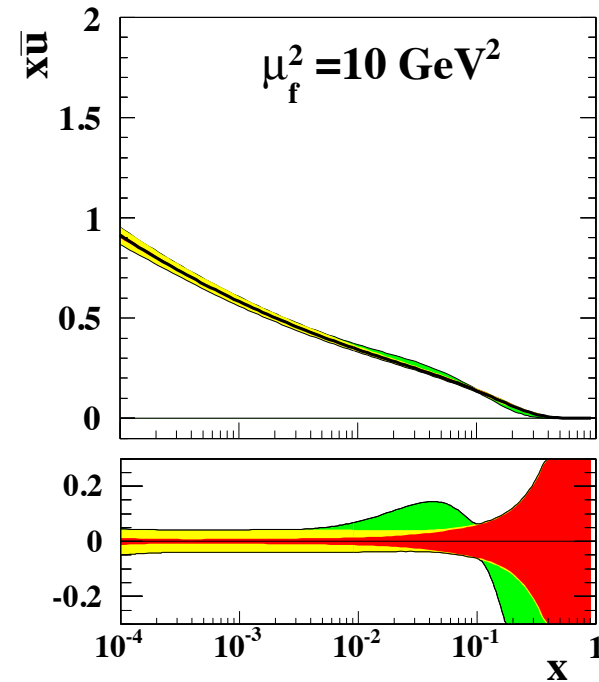
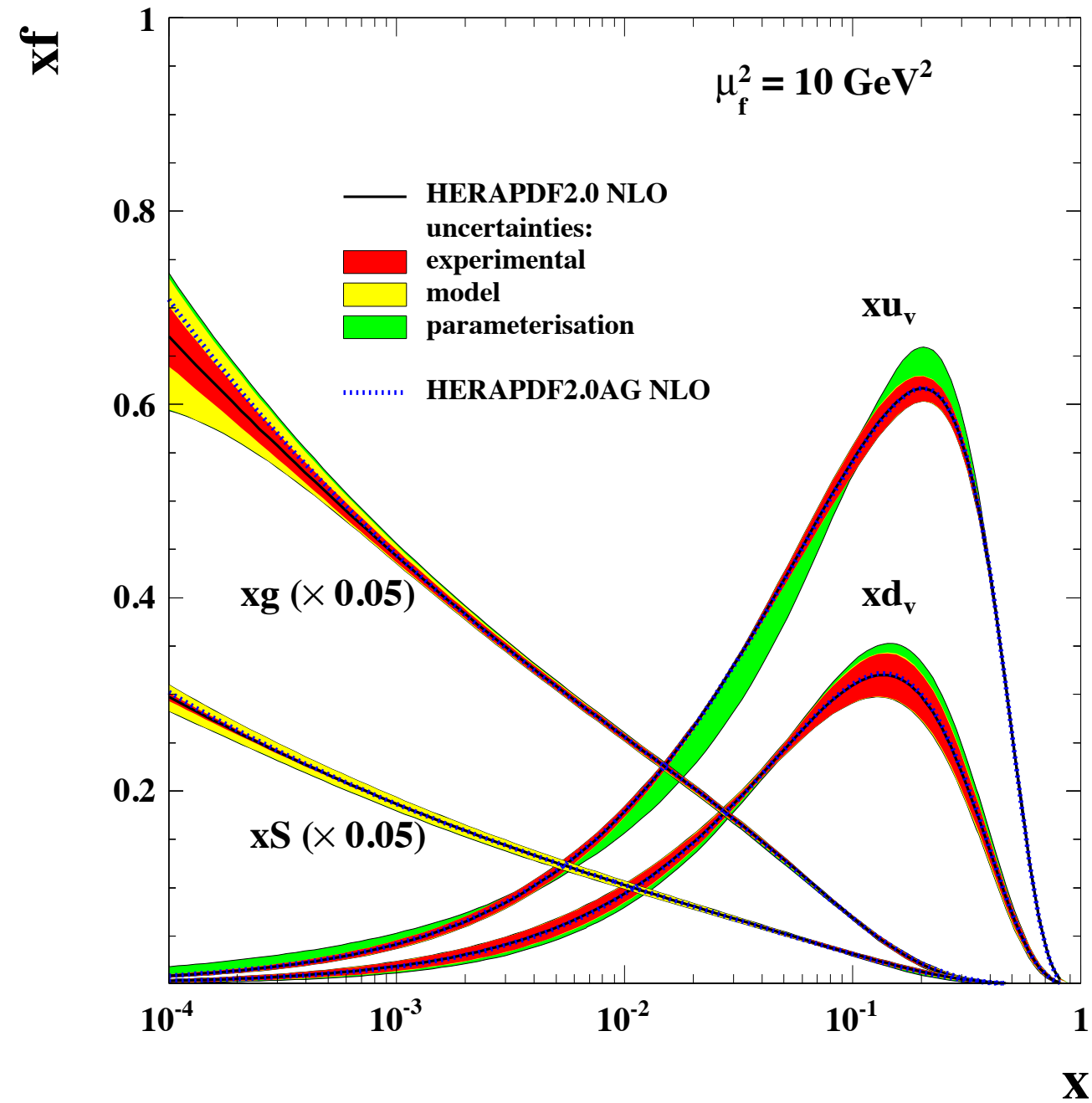
$$\frac{d^2\sigma_{CC}^+}{dx dQ^2} = \frac{G_F^2}{2\pi} \left(\frac{M_W^2}{M_W^2 + Q^2} \right)^2 \left[(\bar{u} + \bar{c}) + (1 - y)^2 (d + s) \right]$$

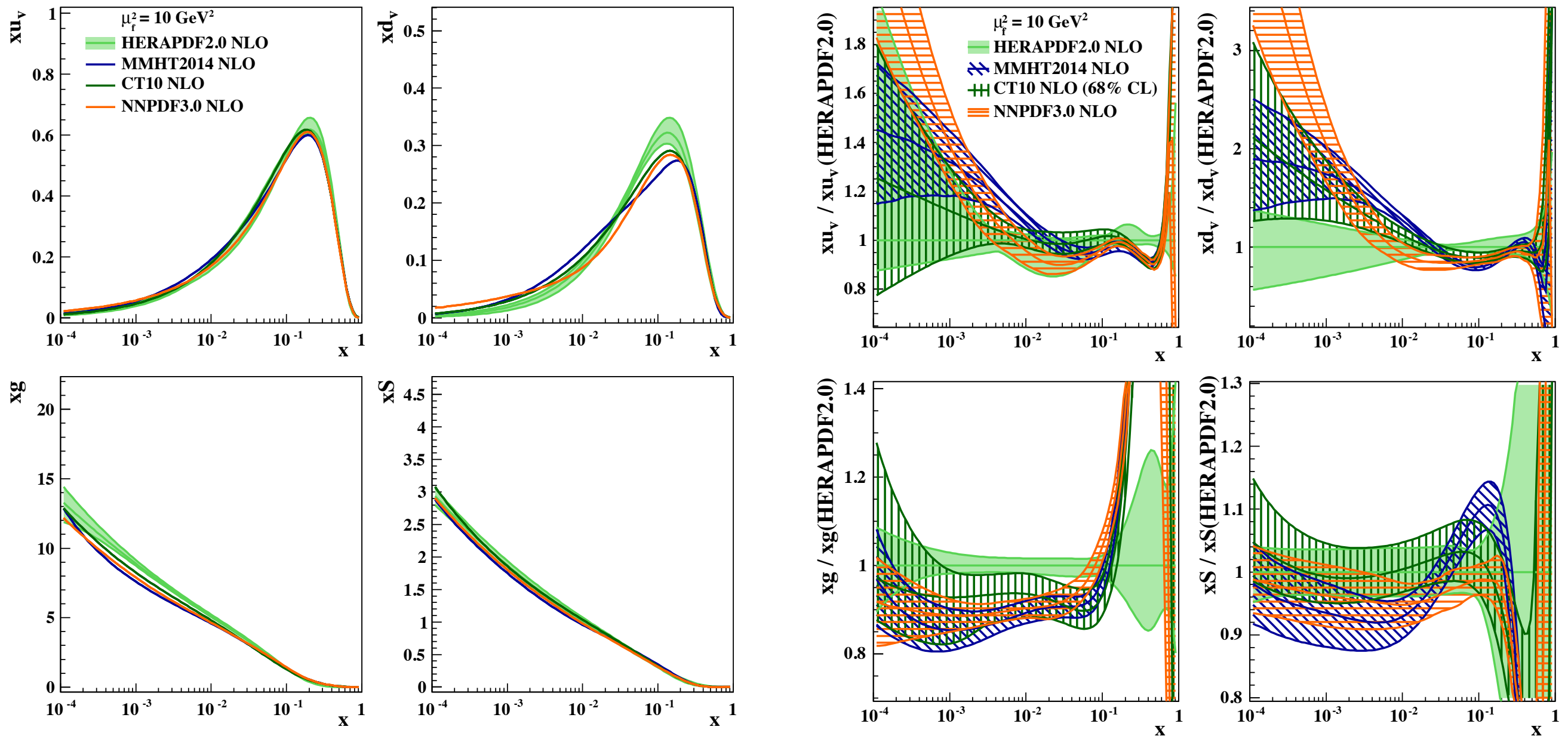


Combination of high Q^2 CC data (HERA-I+II)
 Improvement of total uncertainty
 Dominated by statistical errors
 Provide important flavour decomposition information



CC e^+ data provide strong d_v constraint at high x
 Precision limited by statistics: typically 3-7%
 HERA-I precision of 10-15% for e^+p





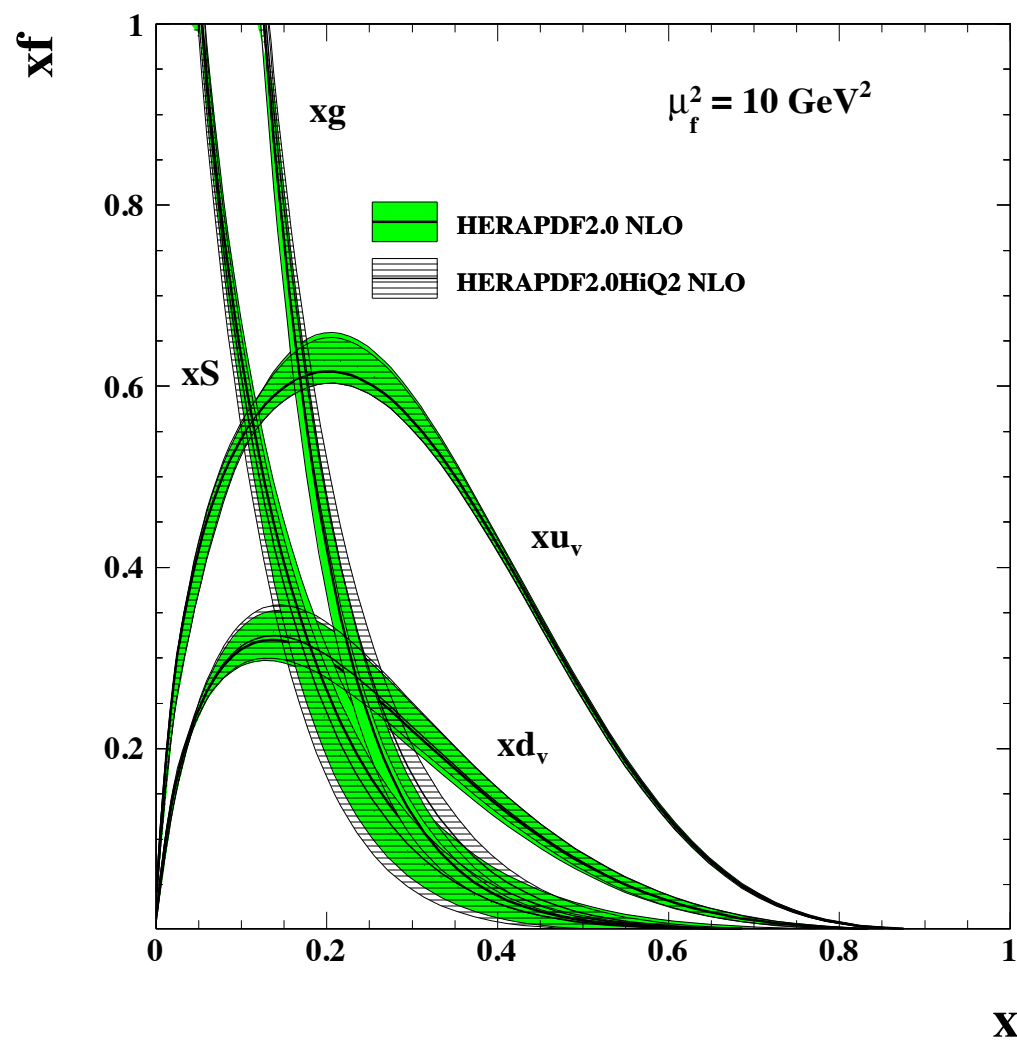
Comparison of HERAPDF2.0 vs MMHT14 , NNPDF3.0 , CT10 (others use only HERA-1 combined data)

Differences at high x

- New HERA combined data improve precision at high x , Q^2
- HERAPDF uses proton target data only \rightarrow no nucleon / deuterium data
- Softer gluon at high x

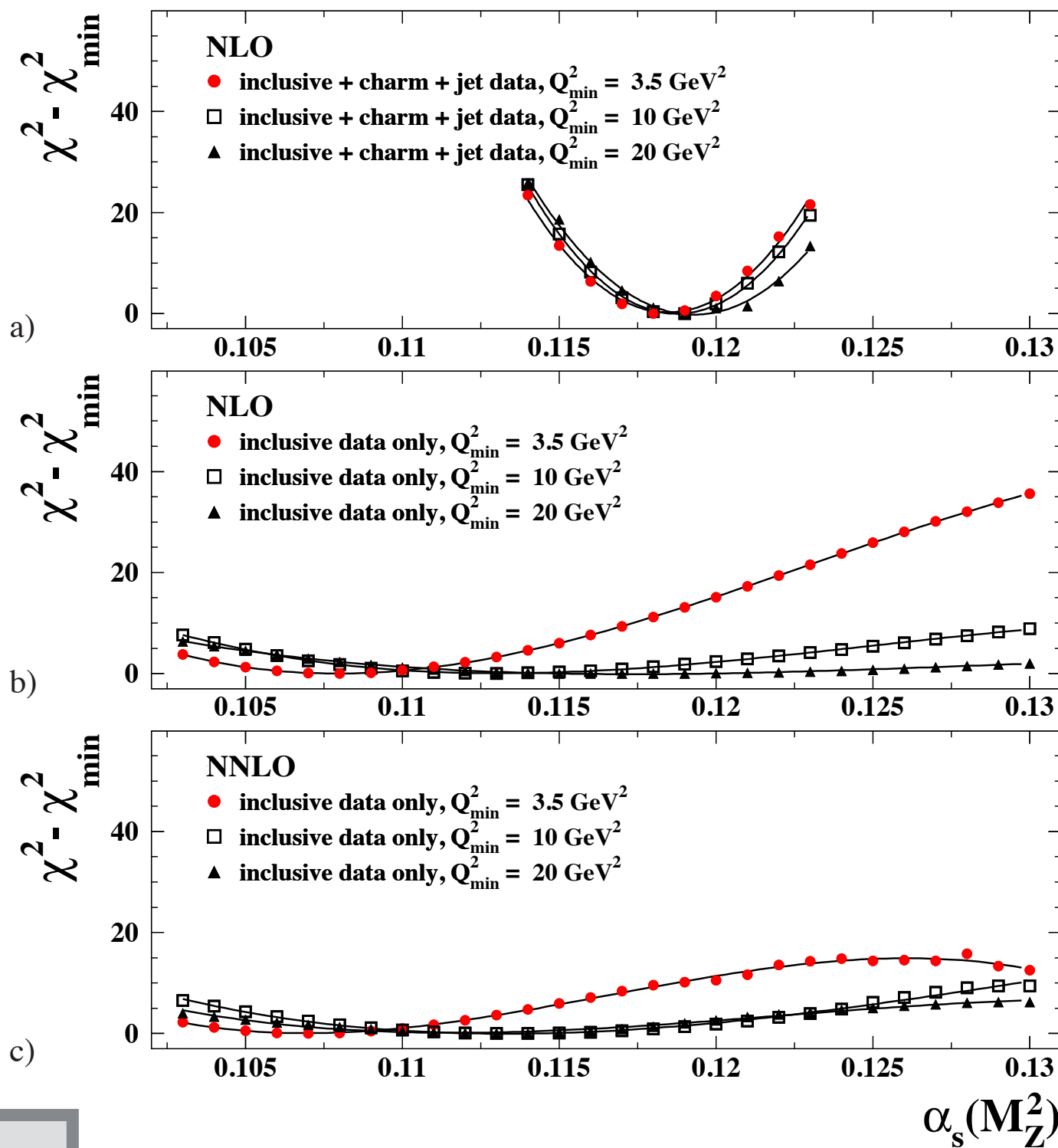
Inclusive jet + charm cross sections in ep collisions are sensitive to xg and α_s

Separate H1 & ZEUS measurements are added to HERAPDF2.0 \rightarrow HERAPDF2.0-Jets



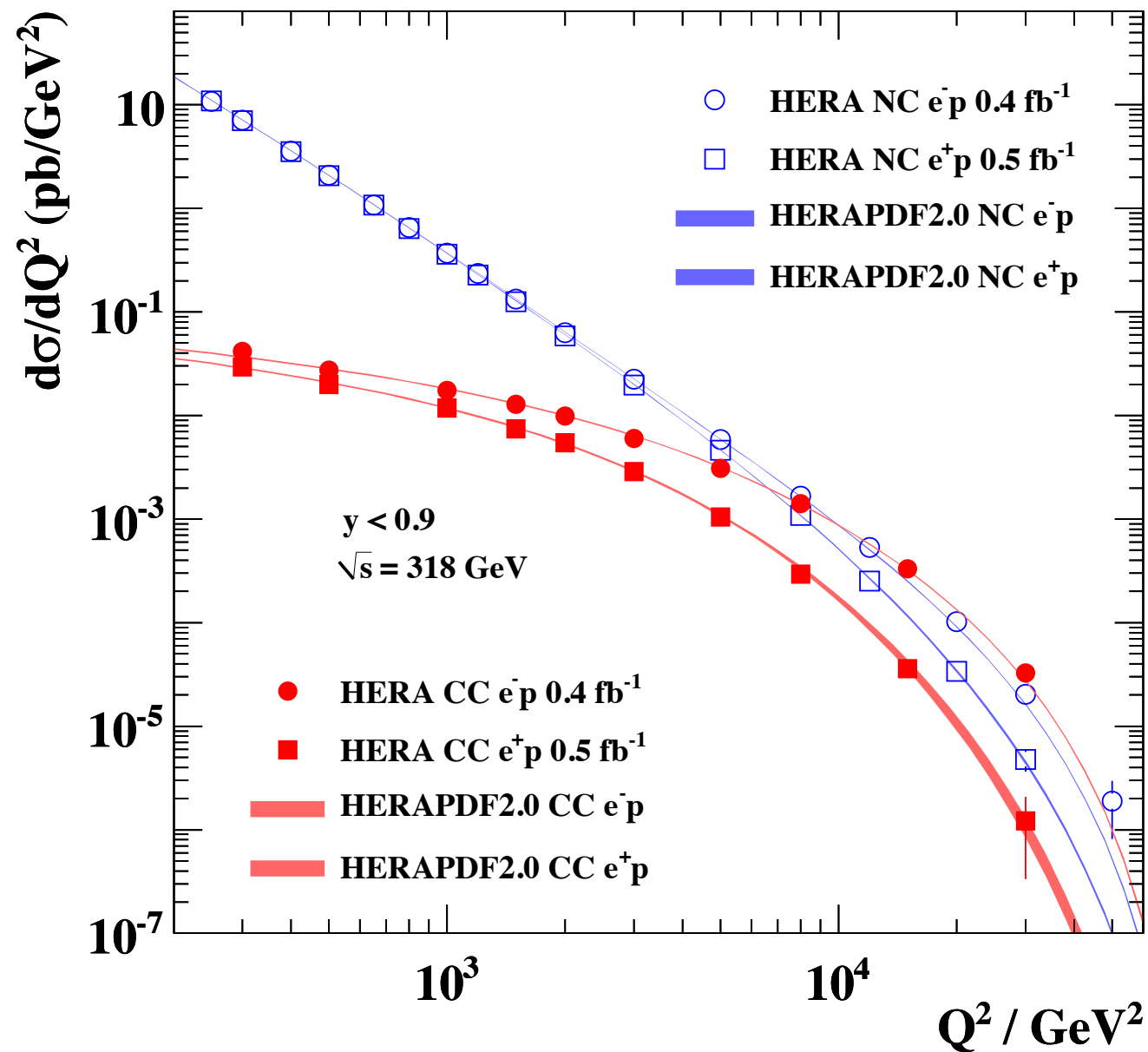
Value of α_s determined from DIS data:

$$\alpha_s(M_Z^2) = 0.1183 \pm 0.0009(\text{exp}) \pm 0.0005(\text{model/parameterisation}) \pm 0.0012(\text{hadronisation}) \begin{matrix} +0.0037 \\ -0.0030 \end{matrix}(\text{scale}) .$$



Consistent with world average
 Competitive with other NLO determinations

Electroweak symmetry breaking



- H1 / ZEUS completed their final SF measurements
- New HERA-II data provide tighter constraints at high x / Q^2
- These data provide some of the most stringent constraints on PDFs
- Stress-test of QCD over 4 orders of mag. in Q^2
- DGLAP evolution works very well
- HERA data provide a self-consistent data set for complete flavour decomposition of the proton
- Final combination of HERA data completed
- HERAPDF2.0 QCD fit at NLO & NNLO



HERAPDF1.0

Combine NC and CC HERA-I data from H1 & ZEUS
 Complete MSbar NLO fit
 NLO: standard parameterisation with 10 parameters
 $\alpha_s = 0.1176$ (fixed in fit)

HERAPDF1.5

Include additional NC and CC HERA-II data
 Complete MSbar NLO and NNLO fit
 NLO: standard parameterisation with 10 parameters
HERAPDF1.5f
 NNLO: extended fit with 14 parameters

desy-09-158

H1-10-142 / ZEUS-prel-10-018

$$xf(x, Q_0^2) = A \cdot x^B \cdot (1-x)^C \cdot (1 + Dx + Ex^2)$$

xg		xg		$xg(x) = A_g x^{B_g} (1-x)^{C_g},$
xu_v	\longrightarrow	$xU = xu + xc$	\longrightarrow	$xu_v(x) = A_{u_v} x^{B_{u_v}} (1-x)^{C_{u_v}} (1 + E_{u_v} x^2),$
xd_v	\longrightarrow	$xD = xd + xs$	\longrightarrow	$xd_v(x) = A_{d_v} x^{B_{d_v}} (1-x)^{C_{d_v}},$
$x\bar{U}$		$x\bar{U} = x\bar{u} + x\bar{c}$		$x\bar{U}(x) = A_{\bar{U}} x^{B_{\bar{U}}} (1-x)^{C_{\bar{U}}},$
$x\bar{D}$		$x\bar{D} = x\bar{d} + x\bar{s}$		$x\bar{D}(x) = A_{\bar{D}} x^{B_{\bar{D}}} (1-x)^{C_{\bar{D}}},$

$$x\bar{s} = f_s x\bar{D} \text{ strange sea is a fixed fraction } f_s \text{ of } \bar{D} \text{ at } Q_0^2$$

Apply momentum/counting sum rules:

$$\int_0^1 dx \cdot (xu_v + xd_v + x\bar{U} + x\bar{D} + xg) = 1$$

$$\int_0^1 dx \cdot u_v = 2 \quad \int_0^1 dx \cdot d_v = 1$$

Parameter constraints:

$$B_{uv} = B_{dv}$$

$$B_{Ubar} = B_{Dbar}$$

$$\text{sea} = 2 \times (\text{Ubar} + \text{Dbar})$$

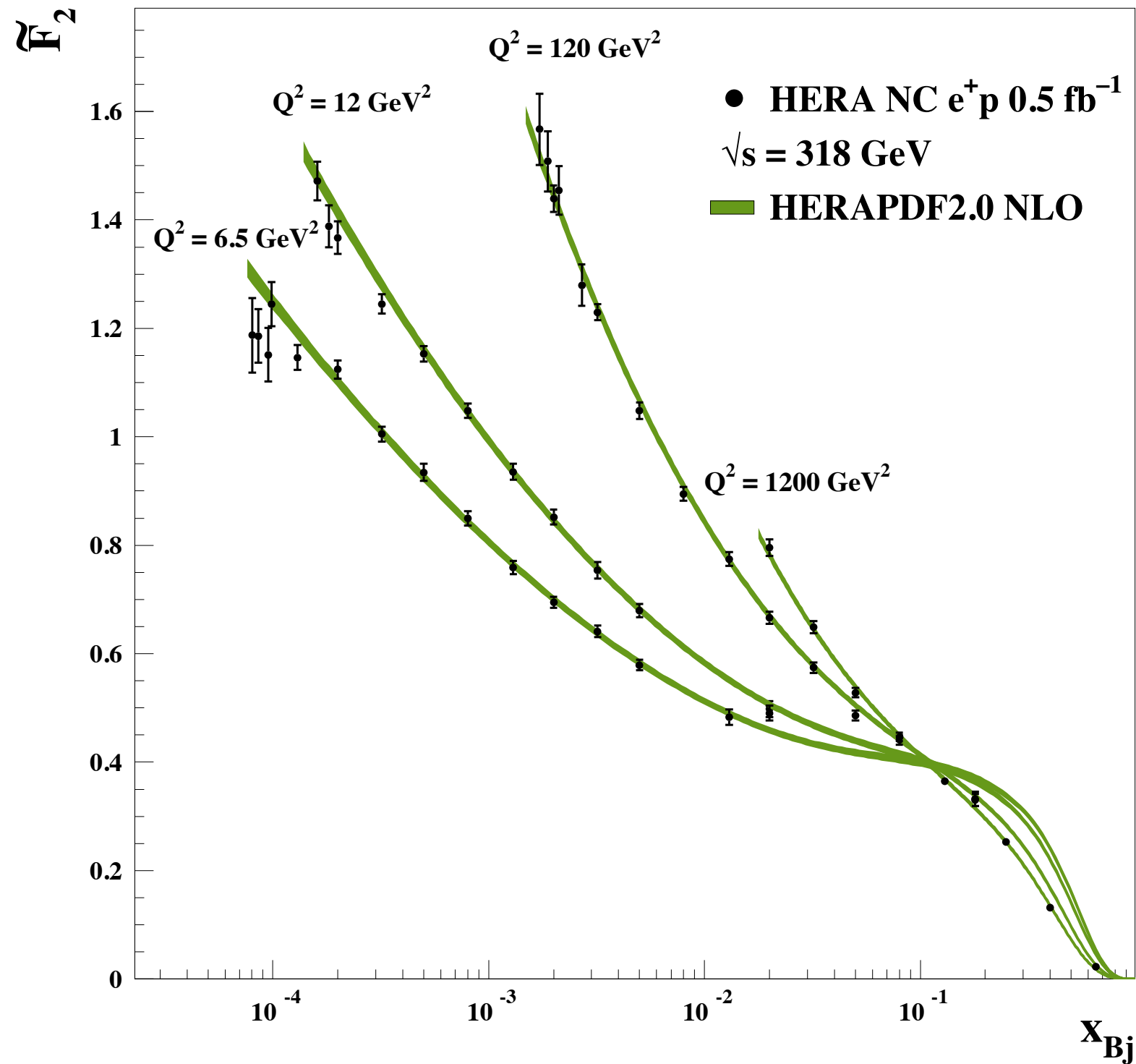
$$\text{Ubar} = \text{Dbar at } x=0$$

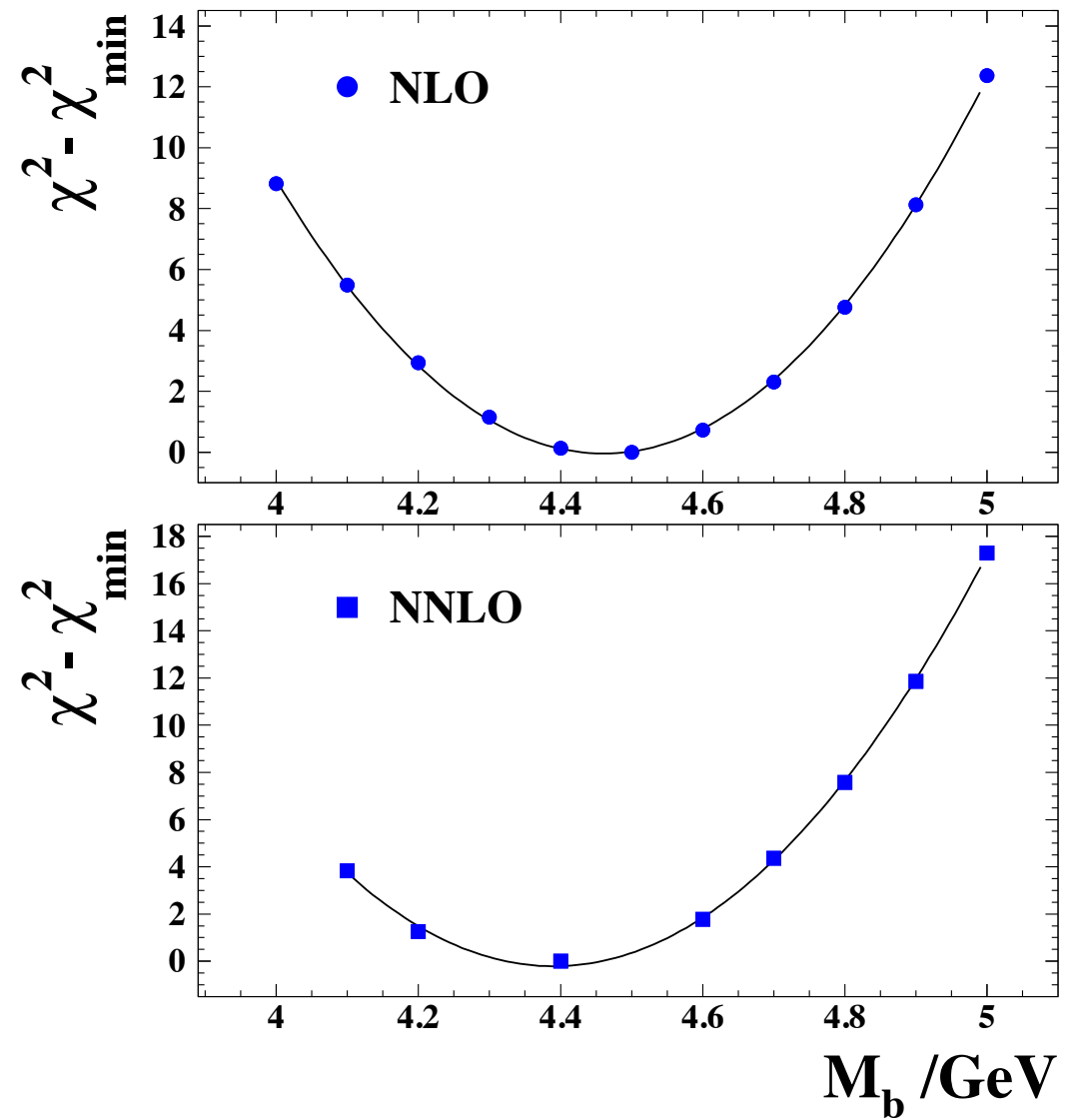
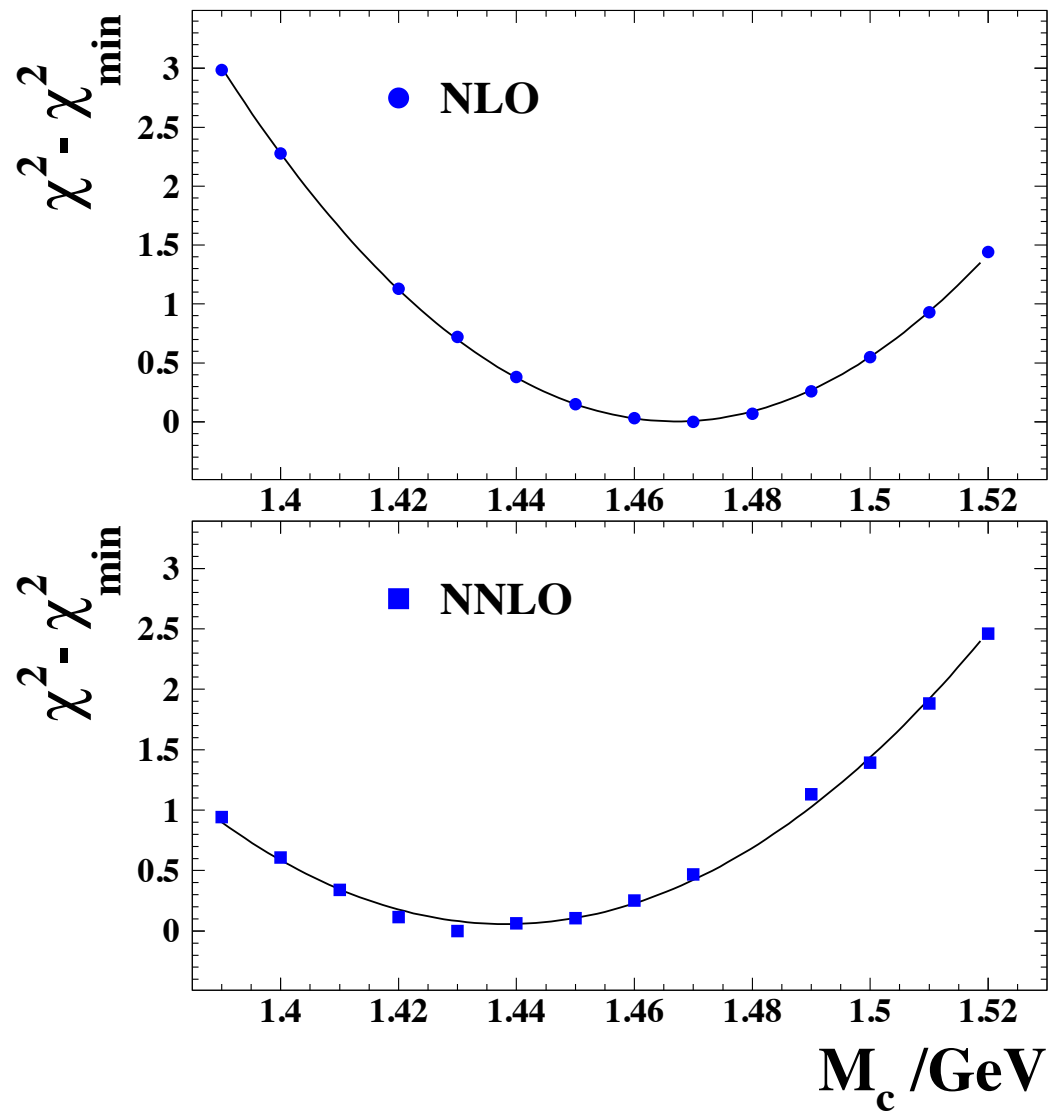
$$Q_0^2 = 1.9 \text{ GeV}^2 \text{ (below } m_c)$$

$$Q^2 > 3.5 \text{ GeV}^2$$

$$2 \times 10^{-4} < x < 0.65$$

Fits performed using RT-VFNS





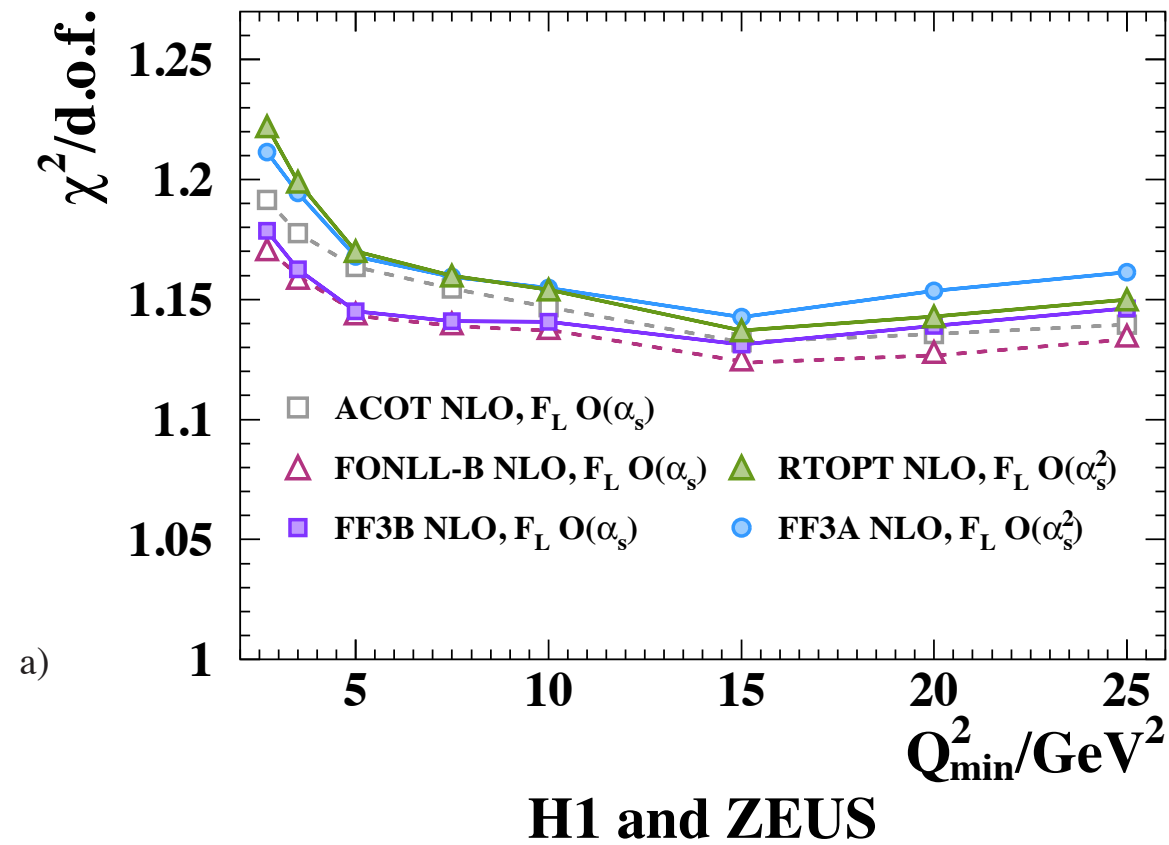
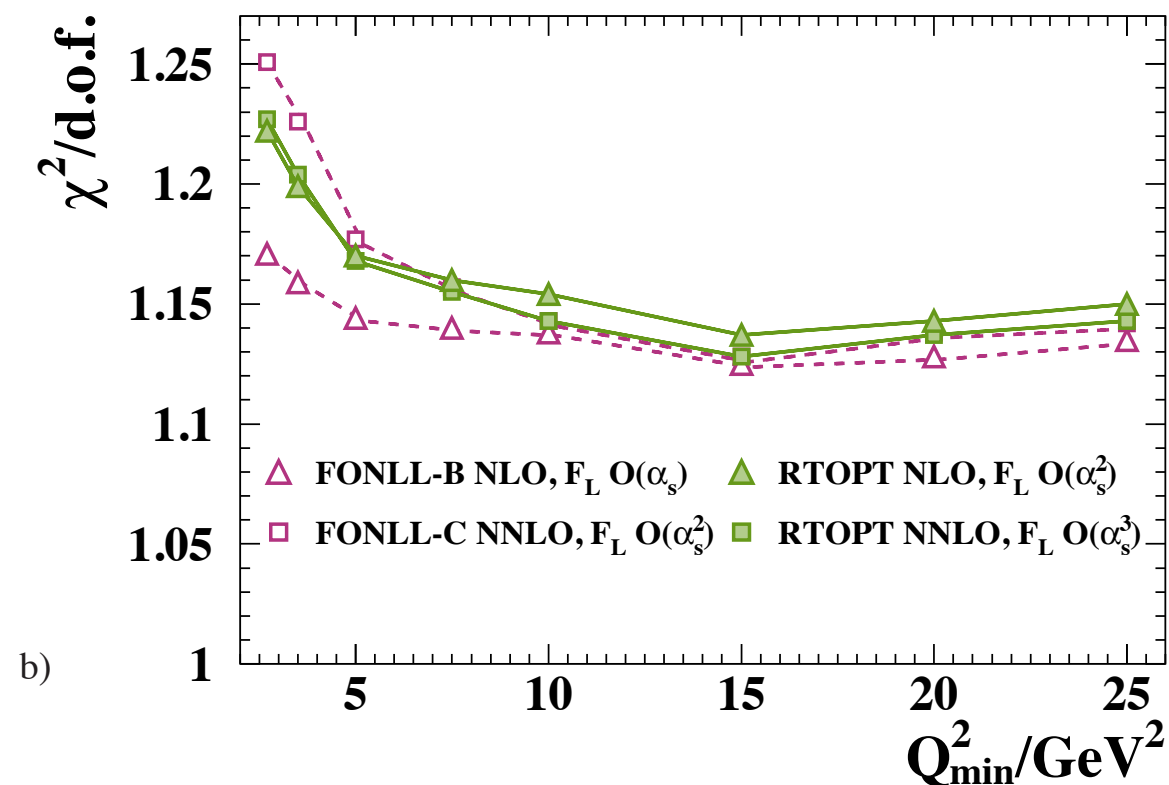
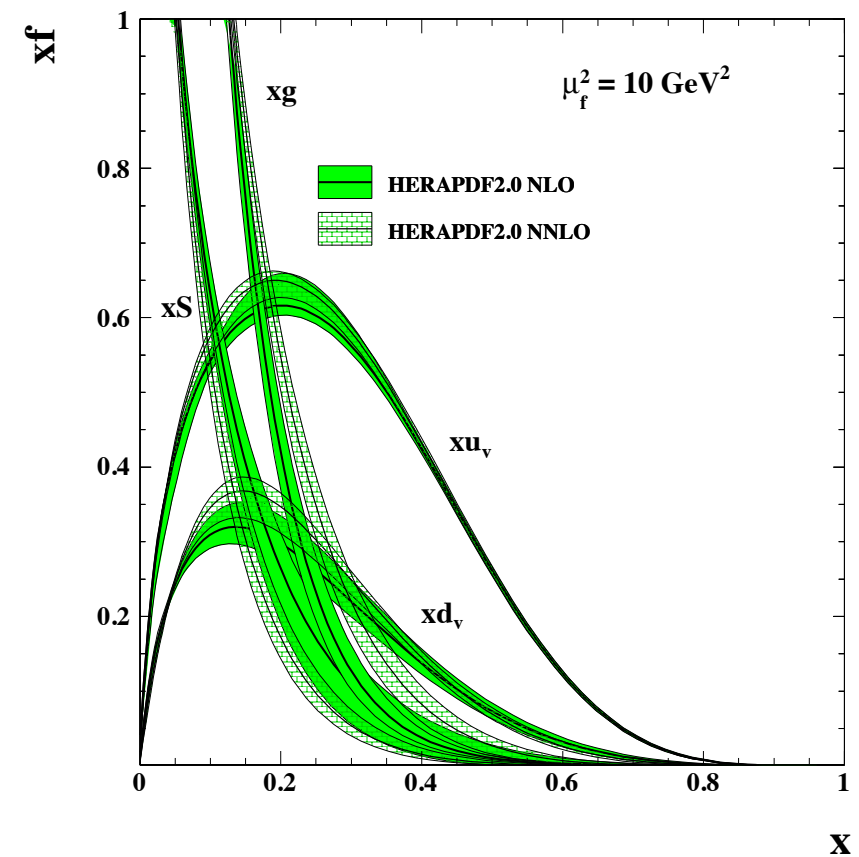
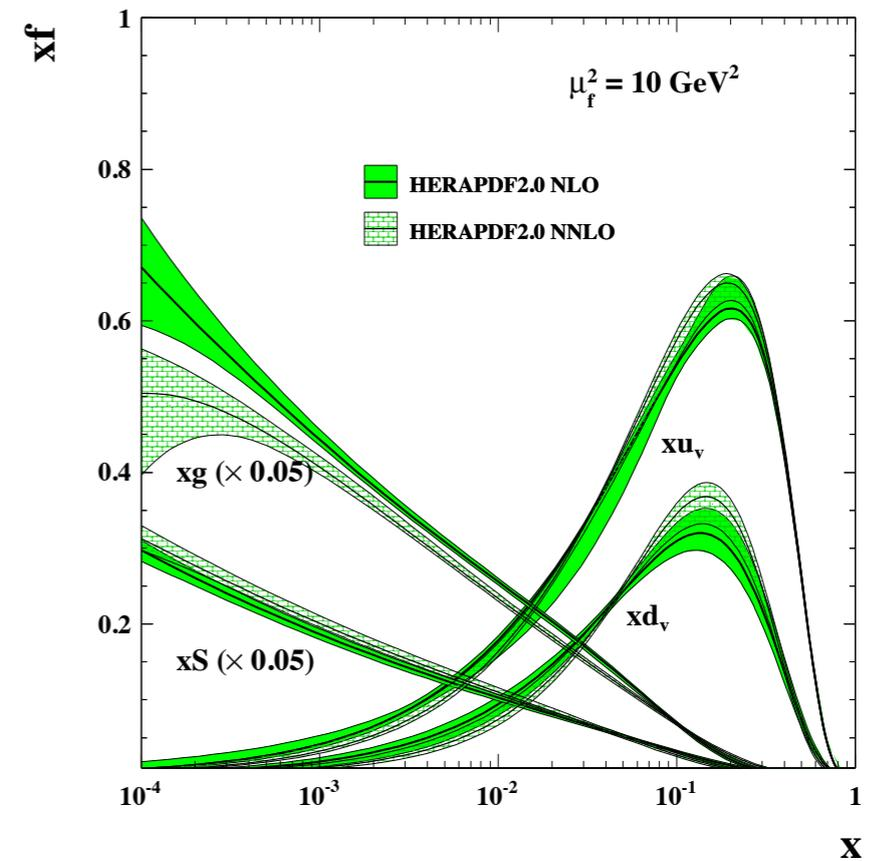
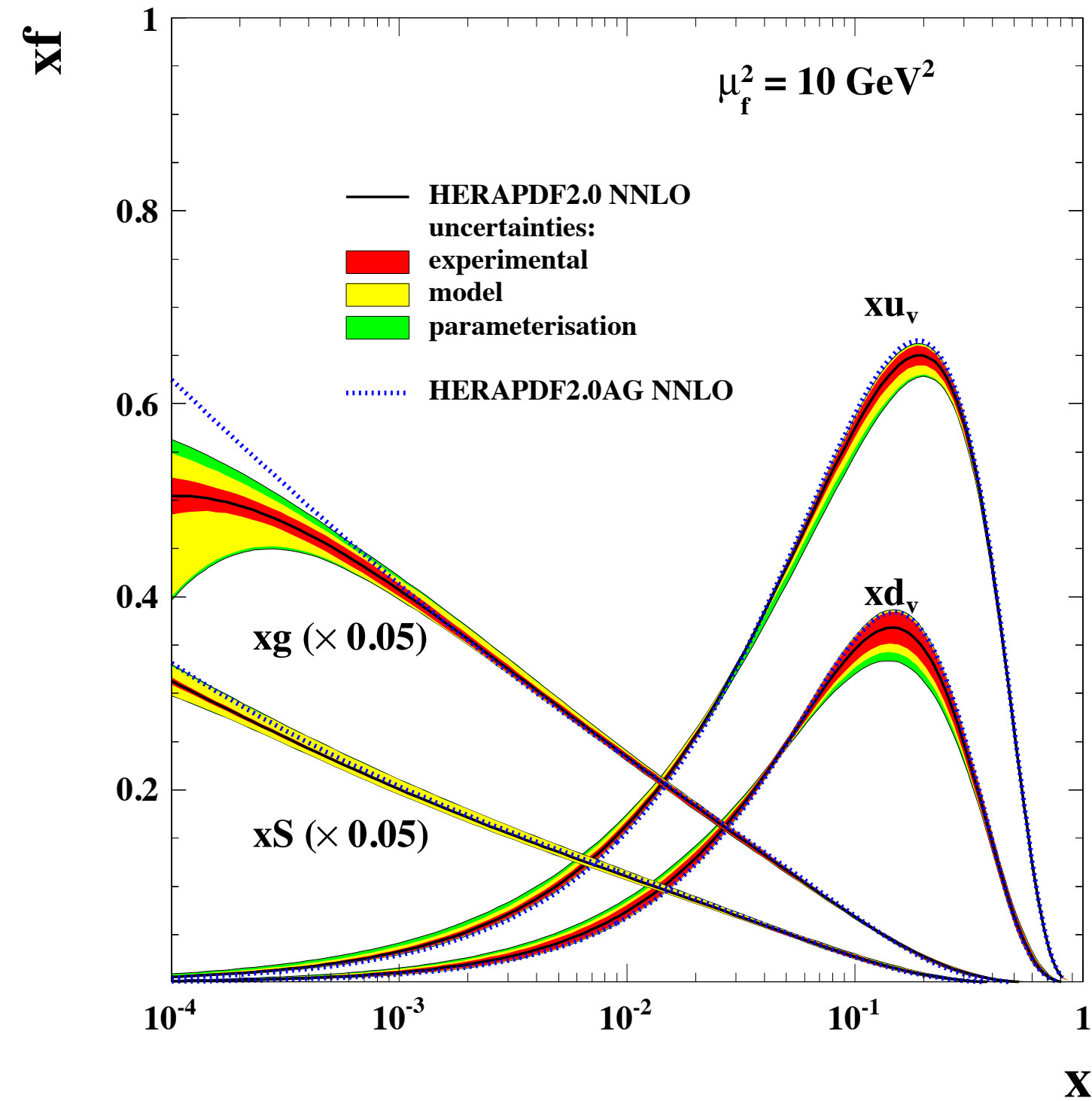


Figure 20: The dependence of $\chi^2/\text{d.o.f.}$ on Q^2_{\min} for HERAPDF2.0 fits using a) the RTOPT [83], FONLL-B [90], ACOT [109] and fixed-flavour (FF) schemes at NLO and b) the RTOPT and FONLL-B/C [91] schemes at NLO and NNLO. The F_L contributions are calculated using matrix elements of the order of α_s indicated in the legend. The number of degrees of freedom drops from 1148 for $Q^2_{\min} = 2.7 \text{ GeV}^2$ to 1131 for the nominal $Q^2_{\min} = 3.5 \text{ GeV}^2$ and to 868 for $Q^2_{\min} = 25 \text{ GeV}^2$.





HERAPDF	$Q_{\min}^2 [\text{GeV}^2]$	χ^2	d.o.f.	$\chi^2/\text{d.o.f}$
2.0 NLO	3.5	1357	1131	1.200
2.0HiQ2 NLO	10.0	1156	1002	1.154
2.0 NNLO	3.5	1363	1131	1.205
2.0HiQ2 NNLO	10.0	1146	1002	1.144
2.0 AG NLO	3.5	1359	1132	1.201
2.0HiQ2 AG NLO	10.0	1161	1003	1.158
2.0 AG NNLO	3.5	1385	1132	1.223
2.0HiQ2 AG NNLO	10.0	1175	1003	1.171
2.0 NLO FF3A	3.5	1351	1131	1.195
2.0 NLO FF3B	3.5	1315	1131	1.163
2.0Jets $\alpha_s(M_Z^2)$ fixed	3.5	1568	1340	1.170
2.0Jets $\alpha_s(M_Z^2)$ free	3.5	1568	1339	1.171

Table 11: The values of χ^2 per degree of freedom for HERAPDF2.0 and its variants.